arXiv:1402.5342v1 [cond-mat.mes-hall] 21 Feb 2014

Scattering nonlocality in quantum charge transport: Application to semiconductor nanostructures

Roberto Rosati and Fausto Rossi*
Department of Applied Science and Technology, Politecnico di Torino
C.so Duca degli Abruzzi 24, 10129 Torino, Italy
(Dated: February 24, 2014)

As discussed in the fundamental solid-state text-book by Neil W. Ashcroft and N. David Mermin, a general and rigorous (i.e. quantum-mechanical) derivation of the standard semiclassical charge-transport theory constitutes a formidable task; indeed, while for homogeneous systems such derivation may be partially simplified, in the general case of a space-dependent carrier system additional approximations are needed, and the validity limits of such a semiclassical description may become highly questionable. Our primary goal is to provide a rigorous treatment of scattering nonlocality in semiconductor nanostructures. On the one hand, starting from the conventional density-matrix formulation and employing as ideal instrument for the study of the semiclassical limit the well-known Wigner-function picture, we shall perform a fully quantum-mechanical derivation of the space-dependent Boltzmann equation. On the other hand, we shall examine the validity limits of such semiclassical framework, pointing out, in particular, regimes where scattering-nonlocality effects may play a relevant role; to this end we shall supplement our analytical investigation with a number of simulated experiments, discussing and further expanding preliminary studies of scattering-induced quantum diffusion in GaN-based nanomaterials. As for the case of carrier-carrier relaxation in photoexcited semiconductors, our analysis will show the failure of simplified dephasing models in describing phonon-induced scattering nonlocality, pointing out that such limitation is particularly severe for the case of quasielastic dissipation processes.

PACS numbers: 72.10.-d, 73.63.-b, 85.35.-p

I. INTRODUCTION

Since the seminal paper by Esaki and Tsu,[1] artificially tailored as well as self-assembled semiconducting nanostructures[2] form the leading edge of semiconductor science and technology.[3–5] The design of state-of-the-art optoelectronic devices, in fact, heavily exploits the principles of band-gap engineering,[6] achieved by confining charge carriers in spatial regions comparable to their de Broglie wavelengths.[7] This, together with the progressive reduction of the typical time-scales involved, pushes device miniaturization toward limits where the application of the traditional Boltzmann transport theory[8] becomes questionable, and a comparison with more rigorous quantum-transport approaches[9–15] is imperative. However, in spite of the quantum-mechanical nature of electron and photon dynamics in the core regions of typical solid-state nanodevices (e.g., quantum dots[16,17] and graphene-based structures[18,19]) the overall behavior of such quantum systems is often governed by a highly non-trivial interplay between phase coherence and dissipation/dephasing.[20]

In spite of the intrinsic validity limits just recalled, during the last decades a number of Boltzmann-like Monte Carlo simulation schemes have been extensively employed for the investigation of new-generation semiconductor nanodevices.[21–32] Such modeling strategies — based on the neglect of carrier phase coherence— are however unable to properly describe space-dependent ultrafast phenomena. To this aim, the crucial step is to adopt a quantum-mechanical description of the carrier subsystem; this can be performed at different levels, ranging from phenomenological dissipation/decoherence models[33] to quantum-kinetic treatments.[10,12,13] Indeed, in order to overcome the intrinsic limitations of the semiclassical picture in properly describing ultrafast space-dependent phenomena —e.g., real-space transfer and escape versus capture processes— Jacoboni and co-workers have proposed a quantum Monte Carlo technique,[34] while Kuhn and co-workers have proposed a quantum-kinetic treatment;[35] however, due to their high computational cost, these non-Markovian density-matrix approaches are currently unsuitable for the design and optimization of new-generation nanodevices.

In order to overcome such limitations, a conceptually simple as well as physically reliable quantum-mechanical generalization of the conventional Boltzmann theory has been recently proposed.[36] The latter preserves the power and flexibility of the semiclassical picture in describing a large variety of scattering mechanisms; more specifically, employing a microscopic derivation of generalized scattering rates based on a recent reformulation of the Markov limit,[37] a density-matrix equation has been derived, able to properly account for space-dependent ultrafast dynamics in semiconductor nanostructures in the low-carrier-density regime; indeed, the density-matrix approach proposed in Ref. 36 has been recently applied to the analysis of genuine quantum-diffusion phenomena in GaN-based bulk and nanostructured materials,[38] allowing for a preliminary analysis of free-carrier versus scattering-induced diffusion.

Primary goal of this paper is to provide a rigorous treatment of scattering nonlocality. On the one

hand, starting from the conventional density-matrix formulation[39,40] and employing as ideal instrument for the study of the semiclassical limit the well-known Wigner-function picture,[39,41] we shall perform a fully quantum-mechanical derivation of the space-dependent Boltzmann equation. On the other hand, we shall examine the validity limits of such semiclassical approximation scheme, pointing out, in particular, regimes where scattering-nonlocality effects may play a relevant role; to this end we shall supplement our analytical investigation with a number of simulated experiments, discussing and further expanding the preliminary study of scattering-induced quantum diffusion in GaN-based nanomaterials recently presented in Ref. 38. As for the case of carrier-carrier relaxation in photoexcited semiconductors,[12] our analysis will show the failure of simplified dephasing models in describing phonon-induced scattering nonlocality, pointing out that such limitation is particularly severe for the case of quasielastic dissipation processes.

The Paper is organized as follows: In Sect. II we shall recall the fundamentals of the well-established semiclassical or Boltzmann transport theory applied to bulk semiconductor materials, stressing the basic approximations involved and the corresponding application limits. Sect. III is devoted to the basic concepts and instruments commonly employed for the microscopic investigation of high-field transport and/or ultrafast optical excitations in semiconductor materials in terms of the single-particle density-matrix formalism. In Sect. IV we shall introduce the well-known Wigner-function picture; the latter —often regarded as a classical-like phase-space representation of quantum mechanics— will allows us to identify the general approximation scheme needed in order to derive the conventional space-dependent Boltzmann equation from the density-matrix formalism. Thanks to a few prototypical simulated experiments, in Sect. V we shall be able to identify conditions where scattering-nonlocality effects —absent within the semiclassical treatment— may play a crucial role. Finally, in Sec. VI we shall summarize and draw a few conclusions.

II. THE SEMICLASSICAL OR BOLTZMANN THEORY

The starting point of the so-called semiclassical picture recalled in this section is the well-known Boltzmann equation,[42–44] an integro-differential equation proposed at the end of the 19-th century by Ludwig Boltzmann in his kinetic theory of gases.[45] Goal of such equation was the description of nonequilibrium diffusion as well as transport phenomena for a generic gas of N point-like classical particles, whose phase-space distribution is described via a single-particle picture in terms of the so-called distribution function $f(\mathbf{r},\mathbf{p})$, proportional to the probability of finding a particle with position $\mathbf{r}$ and momentum $\mathbf{p}$. Each particle will evolve according to the corresponding single-particle Hamilton equations, but it will also undergo stochastic collision processes with other particles. The Boltzmann equation is the equation of motion for the distribution function: by denoting with $\mathbf{F}$ the classical force corresponding to an external single-particle potential $V(\mathbf{r})$ and employing the equations of motion

$$\dot{\mathbf{r}} = \frac{\mathbf{p}}{m} \ , \qquad \dot{\mathbf{p}} = \mathbf{F} \tag{1}$$

corresponding to the single-particle Hamiltonian

$$H(\mathbf{r},\mathbf{p}) = \frac{p^2}{2m} + V(\mathbf{r}) \ , \tag{2}$$

one gets

$$\frac{\partial f}{\partial t} + \frac{\mathbf{p}}{m}\cdot\frac{\partial f}{\partial \mathbf{r}} + \mathbf{F}\cdot\frac{\partial f}{\partial \mathbf{p}} = \left.\frac{\partial f}{\partial t}\right|_{\rm scat} \tag{3}$$

with

$$\left.\frac{\partial f}{\partial t}\right|_{\rm scat} = \int d^3p' \left[W(\mathbf{p},\mathbf{p}')f(\mathbf{r},\mathbf{p}') - W(\mathbf{p}',\mathbf{p})f(\mathbf{r},\mathbf{p})\right] \ . \tag{4}$$

The Boltzmann equation (3) simply states that the total time variation of the distribution function due to the deterministic single-particle motion is equal to the corresponding variation due to particle-particle scattering; the latter are described via the so-called "collision term" in (4), whose physical interpretation is straightforward: denoting with $W(\mathbf{p}',\mathbf{p})$ the collision or scattering probability per time unit from $\mathbf{p}$ to $\mathbf{p}'$, the net variation of f at the current phase-space point $\mathbf{r},\mathbf{p}$ is given by all particles scattered from any $\mathbf{p}'$ into the current value $\mathbf{p}$ ("in-scattering" contribution) minus all particles scattered out of $\mathbf{p}$ to any value $\mathbf{p}'$ ("out-scattering" contribution). Within the Boltzmann kinetic theory, such collision processes are assumed to be instantaneous and point-like,[44] i.e., $\mathbf{r},\mathbf{p} \to \mathbf{r},\mathbf{p}'$.

Under suitable physical conditions, such purely classical transport theory may be successfully employed for the description of non-classical systems; this constitutes the essence of the so-called semiclassical picture. Indeed, in spite of its unambiguous quantum-mechanical nature, the behavior of a Bloch electron with wavevector $\mathbf{k}$ subjected to a slowly-varying electromagnetic force may be described via a classical particle of momentum $\mathbf{p} = \hbar\mathbf{k}$. More precisely, the crucial idea is to describe the electronic state in a given crystal band via a wavepacket characterized by a central (or reference) position $\mathbf{r}$ and momentum $\mathbf{p}$; in the presence of a slowly-varying applied force $\mathbf{F}$, it is possible to show that the time evolution of the wavepacket reference coordinates $\mathbf{r},\mathbf{p}$ is dictated by the following semiclassical equations of motion

$$\dot{\mathbf{r}} = \mathbf{v} \ , \qquad \dot{\mathbf{p}} = \mathbf{F} \tag{5}$$

corresponding to the effective crystal Hamiltonian

$$H_{\rm sp}(\mathbf{r},\mathbf{p}) = K(\mathbf{p}) + V(\mathbf{r}) \ . \tag{6}$$

Compared to the classical Hamilton equations (1), here the particle velocity $\frac{\mathbf{p}}{m}$ is replaced by the so-called carrier group velocity ($\mathbf{v} = \frac{\partial K}{\partial \mathbf{p}}$) defined as the $\mathbf{p}$-gradient of the electronic energy band $K(\mathbf{p})$.

Such a particle-like description may be employed provided to fulfill the uncertainty principle: $\Delta r \Delta p \geq \frac{\hbar}{2}$; this means that such semiclassical picture is expected to become inadequate on very short space-scales, as we shall discuss in more detail in Sec. IV.

In analogy with the kinetic theory of gases previously recalled, we shall introduce a corresponding distribution function $f(\mathbf{r}, \mathbf{p})$,[8,20,46] describing the probability of finding an electron with Bloch quasimomentum $\mathbf{p} = \hbar\mathbf{k}$ and position $\vec{r}$. By employing the semiclassical result in (5), it is easy to derive the following electronic-transport equation

$$\frac{\partial f}{\partial t} + \mathbf{v} \cdot \frac{\partial f}{\partial \mathbf{r}} + \mathbf{F} \cdot \frac{\partial f}{\partial \mathbf{p}} = \left. \frac{\partial f}{\partial t} \right|_{\text{scat}} \tag{7}$$

with a semiclassical collision or scattering term formally identical to the one in (4):

$$\left. \frac{\partial f}{\partial t} \right|_{\text{scat}} = \int d^3p' \left[P(\mathbf{p}, \mathbf{p}') f(\mathbf{r}, \mathbf{p}') - P(\mathbf{p}', \mathbf{p}) f(\mathbf{r}, \mathbf{p}) \right] . \tag{8}$$

with

$$P(\mathbf{p}, \mathbf{p}') = \sum_s P^s(\mathbf{p}, \mathbf{p}') . \tag{9}$$

Here, the scattering rates $P^s(\mathbf{p}, \mathbf{p}')$ describe again instantaneous and point-like scattering processes $(\mathbf{r}, \mathbf{p}' \rightarrow \mathbf{r}, \mathbf{p})$ induced by the generic interaction mechanism s; compared to the original Boltzmann collision term in (4), in addition to inter-particle (carrier-carrier) scattering, our Bloch electrons will undergo stochastic transitions induced by a number of interaction mechanisms ascribed to the host material, like, e.g., carrier-phonon, carrier-plasmon, carrier-impurity scattering, etc.

Compared to the purely classical Boltzmann equation (3), the electronic-transport equation (7) is semiclassical in nature, i.e., it is grounded on the following quantum-mechanical ingredients: (i) the electron group velocity $\mathbf{v}$ (see Eq. (5)) and (ii) the microscopic scattering rates $P^s(\mathbf{p}, \mathbf{p}')$. Indeed, the latter are typically derived in quantum-mechanical terms via the well-known Fermi's golden rule; more precisely, in the low-density limit we have

$$P^s(\mathbf{p}, \mathbf{p}') = \frac{\Omega}{(2\pi\hbar)^3} P^s_{\mathbf{p}\mathbf{p}'} , \tag{10}$$

i.e., the (continuous) scattering-rate functions $P^s(\mathbf{p}, \mathbf{p}')$ are given by the density of (discrete) Bloch states $\mathbf{p}$ – corresponding to a suitable crystal normalization volume Ω– times the (discrete) microscopic scattering rates $P^s_{\mathbf{p}\mathbf{p}'}$ derived via the conventional Fermi's golden rule. It is worth stressing that, in general, the scattering rates in (10) may be space-dependent as well; however, according to the validity limits of the semiclassical description, such space variations should be adiabatically slow compared to the quantum-mechanical space-scale. This implies that the crystal normalization volume Ω introduced in Eq. (10) (and involved in the Fermi's-golden-rule calculation of the scattering rates $P^s_{\mathbf{p}\mathbf{p}'}$) should be much larger than the typical carrier coherence length and, at the same time, much smaller than the macroscopic spatial variations of our material. Under such conditions, the scattering rates $P^s_{\mathbf{p}\mathbf{p}'}$ are evaluated treating our system as homogeneous within the normalization volume Ω, parameterizing the key material properties (e.g., carrier and impurity concentrations, etc.) via the spatial coordinate $\mathbf{r}$. As we shall see, such crystal normalization volume Ω comes out to be the coarse-graining space-scale (see Eq. (79)) involved in the quantum-mechanical derivation of the Boltzmann equation, presented in Sec. IV.

In order to better compare the Wigner transport theory introduced in Sec. IV with its semiclassical counterpart, it is convenient to rewrite the Boltzmann transport equation (7) as

$$\frac{\partial f}{\partial t} = \left. \frac{\partial f}{\partial t} \right|_{\text{sp}} + \left. \frac{\partial f}{\partial t} \right|_{\text{scat}} , \tag{11}$$

where

$$\left. \frac{\partial f}{\partial t} \right|_{\text{sp}} = - \left\{ f, H_{\text{sp}} \right\}_{\text{P}} \tag{12}$$

describes the scattering-free evolution in terms of the so-called Poisson brackets of our single-particle phase-space $\mathbf{r}, \mathbf{p}$, namely

$$\{a, b\} \equiv \frac{\partial a}{\partial \mathbf{r}} \cdot \frac{\partial b}{\partial \mathbf{p}} - \frac{\partial b}{\partial \mathbf{r}} \cdot \frac{\partial a}{\partial \mathbf{p}} . \tag{13}$$

Moreover, for any given physical quantity $a(\mathbf{r}, \mathbf{p})$, its average value can be expressed via the distribution function $f(\mathbf{r}, \mathbf{p})$ as the following integral over our semiclassical phase-space $\mathbf{r}, \mathbf{p}$:

$$\langle a \rangle = (2\pi\hbar)^{-3} \int d\mathbf{r} d\mathbf{p} a(\mathbf{r}, \mathbf{p}) f(\mathbf{r}, \mathbf{p}) . \tag{14}$$

As anticipated, one of the key features of the Boltzmann equation is the local character of its scattering dynamics. In order to better formulate this crucial property, it is useful to recall the link between our distribution function $f(\mathbf{r}, \mathbf{p})$ and the corresponding spatial carrier density $n(\mathbf{r})$:

$$n(\mathbf{r}) = (2\pi\hbar)^{-3} \int d^3p \, f(\mathbf{r}, \mathbf{p}) . \tag{15}$$

Combining the above result with the Boltzmann equation in (11), the time evolution of the spatial carrier density can be written as

$$\frac{\partial n(\mathbf{r})}{\partial t} = \left. \frac{\partial n(\mathbf{r})}{\partial t} \right|_{\text{sp}} + \left. \frac{\partial n(\mathbf{r})}{\partial t} \right|_{\text{scat}} . \tag{16}$$

In particular, combining Eqs. (12) and (15), one gets

$$\left.\frac{\partial n(\mathbf{r})}{\partial t}\right|_{\rm sp} = -\nabla\cdot\mathbf{J}(\mathbf{r}) \ , \tag{17}$$

where

$$\mathbf{J}(\mathbf{r}) = (2\pi\hbar)^{-3}\int d^3p\,\mathbf{v}(\mathbf{p})\,f(\mathbf{r},\mathbf{p}) \tag{18}$$

is the carrier current density. Moreover, combining the definition in (15) with the explicit form of the scattering term in (8), it is easy to show that

$$\left.\frac{\partial n(\mathbf{r})}{\partial t}\right|_{\rm scat} = 0 \quad , \tag{19}$$

i.e., regardless of the specific form of the various scattering rates $P^s(\mathbf{p},\mathbf{p}')$, the scattering dynamics has absolutely no effects on the spatial carrier distribution. As we shall discuss in Sec. IV, this peculiar property of the semiclassical transport model is found to be definitely incompatible with the non-local character of quantum-transport treatments.

Combining Eqs. (16), (17), and (19), one finally gets

$$\frac{\partial n(\mathbf{r})}{\partial t} + \nabla\cdot\mathbf{J}(\mathbf{r}) = 0 \ , \tag{20}$$

i.e., also in the presence of scattering processes one recovers the macroscopic charge continuity equation of classical physics.

III. FUNDAMENTALS OF THE SINGLE-PARTICLE DENSITY-MATRIX FORMALISM

In Sec. II we have recalled the basic concepts of the semiclassical picture. The latter is grounded on a number of approximations, whose validity limits may become questionable in the presence of ultrashort space- and time-scales, and genuine quantum-mechanical treatments of the problem are highly desirable.

In order to investigate in fully quantum-mechanical terms the electro-optical response of semiconductor bulk and nanostructured materials, it is crucial to study the time evolution of single-particle quantities, such as the total carrier density, mean kinetic energy, charge current, and so on. In general, such quantities are given by a suitable (quantum-plus-statistical) average of a corresponding (single-particle) operator $\hat{a}$, usually expressed in terms of the single-particle density-matrix operator $\hat{\rho}$ as[20,47]

$$\langle a\rangle = {\rm tr}\left\{\hat{a}\hat{\rho}\right\} \ . \tag{21}$$

It follows that within the Schrödinger picture the crucial step is to analyze the time evolution of the density-matrix operator $\hat{\rho}$, whose equation of motion in the low-density limit is always of the form:[20]

$$\frac{d\hat{\rho}}{dt} = \left.\frac{d\hat{\rho}}{dt}\right|_{\rm sp} + \left.\frac{d\hat{\rho}}{dt}\right|_{\rm scat} \tag{22}$$

where

$$\left.\frac{d\hat{\rho}}{dt}\right|_{\rm sp} = \frac{1}{i\hbar}\left[\hat{H}_{\rm sp},\,\hat{\rho}\right] \tag{23}$$

describes the coherent dynamics dictated by the noninteracting-electron Hamiltonian $\hat{H}_{\rm sp}$ (including elastic single-electron scattering processes) while

$$\left.\frac{d\hat{\rho}}{dt}\right|_{\rm scat} = \Gamma\left(\hat{\rho}\right) \tag{24}$$

is a linear superoperator Γ encoding the energy-dissipative/decoherent scattering mechanisms that electrons experience within the host material.

The above single-particle quantum equation —whose general structure is the same of the semiclassical one in (11)— applies to a variety of physical problems,[20] ranging from quantum-transport phenomena to ultrafast electro-optical processes; however, it is vital to stress that the degree of accuracy of such density-matrix formalism is intimately related to the choice of the scattering superoperator Γ in (24). Indeed, oversimplified approaches accounting for Γ in a phenomenological way or via kinetic treatments based on the conventional Markov limit[48] may lead to the violation of the positive-definite character of the density-matrix operator $\hat{\rho}$, and therefore to unphysical conclusions. To overcome this serious limitation, an alternative Markov procedure has recently been proposed,[37] showing that it is possible to derive a Lindblad-like scattering superoperator of the form

$$\Gamma\left(\hat{\rho}\right) = \sum_s\left(\hat{A}^s\hat{\rho}\hat{A}^{s\dagger} - \frac{1}{2}\left\{\hat{A}^{s\dagger}\hat{A}^s,\hat{\rho}\right\}\right) . \tag{25}$$

According to this alternative adiabatic-decoupling scheme, in the low-density limit for each single-particle interaction mechanism s one is thus able to perform a fully microscopic derivation of a corresponding Lindblad superoperator,[49] thereby preserving the positive-definite character of the density matrix $\hat{\rho}$.

By denoting with $|\alpha\rangle$ the eigenstates of $\hat{H}_{\rm sp}$ (corresponding to the energy spectrum ϵ_α), i.e.,

$$\hat{H}_{\rm sp} = \sum_\alpha |\alpha\rangle\epsilon_\alpha\langle\alpha| \quad , \tag{26}$$

the single-particle density-matrix operator can be expressed in terms of entries $\rho_{\alpha_1\alpha_2}$ as

$$\hat{\rho} = \sum_{\alpha_1\alpha_2}|\alpha_1\rangle\rho_{\alpha_1\alpha_2}\langle\alpha_2| \quad , \tag{27}$$

and the density-matrix equation (22) reduces to

$$\frac{d\rho_{\alpha_1\alpha_2}}{dt} = \frac{\epsilon_{\alpha_1}-\epsilon_{\alpha_2}}{i\hbar}\,\rho_{\alpha_1\alpha_2} + \left.\frac{d\rho_{\alpha_1\alpha_2}}{dt}\right|_{\rm scat} . \tag{28}$$

Such set of coupled equations of motion for the density-matrix elements $\rho_{\alpha_1\alpha_2}$ are usually referred to as the semiconductor Bloch equations.[50] In particular, the diagonal elements ($\rho_{\alpha_1=\alpha_2}$) describe state populations, while non-diagonal contributions ($\rho_{\alpha_1\neq\alpha_2}$) —also referred to as inter-state polarizations— describe quantum-mechanical phase coherence between the single-particle states α_1 and α_2.[20]

By adopting as scattering superoperator the Lindblad-like prescription in (25), the corresponding matrix elements can be conveniently expressed as

$$\left.\frac{d\rho_{\alpha_1\alpha_2}}{dt}\right|_{\rm scat} = \frac{1}{2}\sum_{\alpha_1'\alpha_2'}\left[\mathcal{P}_{\alpha_1\alpha_2,\alpha_1'\alpha_2'}\rho_{\alpha_1'\alpha_2'} - \mathcal{P}^*_{\alpha_1'\alpha_1',\alpha_1\alpha_2'}\rho_{\alpha_2'\alpha_2}\right] + \text{H.c.} \tag{29}$$

(H.c. denoting the Hermitian conjugate) in terms of the generalized scattering rates

$$\mathcal{P}_{\alpha_1\alpha_2,\alpha_1'\alpha_2'} = \sum_s A^s_{\alpha_1\alpha_1'}A^{s*}_{\alpha_2\alpha_2'} \ . \tag{30}$$

In order to investigate the space dependence of the phenomenon under examination —and to compare it to its semiclassical description (see Eqs. (16), (17), and (19)— let us recall the link between our density matrix $\rho_{\alpha_1\alpha_2}$ and the corresponding spatial carrier density, namely

$$n(\mathbf{r}) = \sum_{\alpha_1\alpha_2}\phi_{\alpha_1}(\mathbf{r})\rho_{\alpha_1\alpha_2}\phi^*_{\alpha_2}(\mathbf{r}) \ , \tag{31}$$

where $\phi_\alpha(\mathbf{r}) = \langle\mathbf{r}|\alpha\rangle$ denotes the real-space wavefunction corresponding to the eigenstate $|\alpha\rangle$. Combining the above result with the density-matrix equation (28), the time evolution of the spatial carrier density is again given by Eq. (16) with

$$\left.\frac{\partial n(\mathbf{r})}{\partial t}\right|_{\rm sp} = \frac{1}{i\hbar}\sum_{\alpha_1\alpha_2}\phi_{\alpha_1}(\mathbf{r})(\epsilon_{\alpha_1}-\epsilon_{\alpha_2})\rho_{\alpha_1\alpha_2}\phi^*_{\alpha_2}(\mathbf{r}) \tag{32}$$

and

$$\left.\frac{\partial n(\mathbf{r})}{\partial t}\right|_{\rm scat} = \sum_{\alpha_1\alpha_2}\phi_{\alpha_1}(\mathbf{r})\Gamma(\hat{\rho})_{\alpha_1\alpha_2}\phi^*_{\alpha_2}(\mathbf{r}) \ . \tag{33}$$

In Sec. IV we shall show that, also for the simplest case of a bulk system ($\alpha = \mathbf{p}$), (i) in the presence of a non-parabolic band the single-particle evolution in (32) deviates from its semiclassical counterpart in (17),[51–53] and (ii) the scattering-induced variation in (33) is in general different from zero, i.e., the action of the scattering superoperator is spatially non-local, in clear contrast to the semiclassical result in (19).

At this point a crucial issue is in order, namely the link between the semiclassical Boltzmann theory of Sec. II and the density-matrix formalism recalled so far. As discussed in the fundamental solid-state text-book by Neil W. Ashcroft and N. David Mermin,[54] a general and rigorous (i.e. quantum-mechanical) derivation of the standard semiclassical charge-transport theory constitutes a formidable task. The simplest approach to this tedious problem —usually referred to as the "diagonal limit"— is to neglect all non-diagonal density matrix elements, which implies to assuming a single-particle density matrix of the form

$$\rho_{\alpha_1\alpha_2} = f_{\alpha_1}\delta_{\alpha_1\alpha_2} \ . \tag{34}$$

From a physical point of view, this amounts to assuming that the impact of various energy dissipation/decoherence phenomena (described via the scattering superoperator Γ) is so strong to suppress at any time all inter-state ($\alpha_1 \neq \alpha_2$) quantum-mechanical phase coherence. By inserting the diagonal-limit prescription (34) into Eqs. (28) and (29), it is easy to get the following equation of motion for the state population f_α:

$$\frac{df_\alpha}{dt} = \sum_{\alpha'}\left[P_{\alpha\alpha'}f_{\alpha'} - P_{\alpha'\alpha}f_\alpha\right] \tag{35}$$

with

$$P_{\alpha\alpha'} = \mathcal{P}_{\alpha\alpha,\alpha'\alpha'} = \sum_s |A^s_{\alpha\alpha'}|^2 \ . \tag{36}$$

Equation (35) is Boltzmann-like, i.e., the time evolution of the carrier population f_α is dictated by a standard (in-minus-out) collision term involving scattering rates $P_{\alpha\alpha'}$ given by the diagonal elements ($\alpha_1\alpha_1' = \alpha_2\alpha_2'$) of the generalized scattering rates in (30). As mentioned previously, by adopting the alternative Markov procedure proposed in Ref. 37, for any given single-particle interaction mechanism s one is able to perform a fully microscopic derivation of the corresponding Lindblad operator $\hat{A}^s$ entering the scattering superoperator (25). Moreover, according to this derivation, the diagonal elements of the generalized scattering rates in (36) are given by the conventional Fermi's golden rule. Indeed, the Boltzmann-like equation in (35) can be regarded as the formal justification and starting point of a wide variety of Monte Carlo simulations of charge transport in semiconductor nanostructures, whose main microscopic ingredients are the carrier wavefunctions $\phi_\alpha(\mathbf{r})$ as well as the corresponding scattering rates $P_{\alpha\alpha'}$ obtained via the Fermi's golden rule.

In spite of the success of such Boltzmann-like treatment applied to the study of the steady-state electro-optical response of semiconductor nanodevices,[21–32] the

latter is not able to describe the time-dependent evolution of the spatial carrier density. Indeed, by inserting the diagonal prescription (34) into Eq. (32), the single particle contribution to the spatial carrier density is always equal to zero. This implies that such diagonal approximation does not allow one to account for the diffusion dynamics of the semiclassical transport theory (see Eq. (17)). This can be easily understood noticing that within the diagonal approximation the spatial carrier density in (31) reduces to

$$n(\mathbf{r}) = \sum_{\alpha} |\phi_{\alpha}(\mathbf{r})|^2 \, f_{\alpha} \ . \tag{37}$$

This tells us that for the particular case of a bulk system —the one considered in the semiclassical theory of Sec. II— the single-particle basis states $|\alpha\rangle$ are momentum eigenstates, whose probability density $|\psi_{\alpha}(\mathbf{r})|^2$ is space-independent. It follows that for a bulk system the carrier density $n(\mathbf{r})$ corresponding to the above diagonal-limit picture is space-independent as well.

The obvious conclusion is that the diagonal-approximation scheme just recalled does not allow one to recover the space-dependent Boltzmann theory of Sec. II. Indeed, to this end it is vital to adopt an alternative treatment able to preserve a space-dependent description of the problem; this may be conveniently performed via the well-known Wigner picture discussed below.[55]

IV. THE WIGNER-FUNCTION PICTURE AND THE SEMICLASSICAL LIMIT

A. The Wigner transport equation

As anticipated, in order to account for the space-dependent character of a generic quantum nanomaterial/nanodevice and to properly identify its semiclassical limit, a commonly employed strategy is the Wigner-function treatment of the problem.[9,56] The Wigner function $f^{\rm W}(\mathbf{r},\mathbf{p})$ associated to a single-particle density-matrix operator $\hat{\rho}$ is defined as its Weyl-Wigner transform

$$\begin{aligned} f^{\rm W}(\mathbf{r},\mathbf{p}) &= \int d\mathbf{r}' e^{\frac{\mathbf{p}\cdot\mathbf{r}'}{i\hbar}} \left\langle \mathbf{r}+\frac{\mathbf{r}'}{2}\right| \hat{\rho} \left|\mathbf{r}-\frac{\mathbf{r}'}{2}\right\rangle \\ &= {\rm tr}\{\hat{W}(\mathbf{r},\mathbf{p})\hat{\rho}\} \ , \end{aligned} \tag{38}$$

corresponding to the quantum-plus-statistical average of the Wigner operator[20]

$$\hat{W}(\mathbf{r},\mathbf{p}) = \int d\mathbf{r}' \left|\mathbf{r}-\frac{\mathbf{r}'}{2}\right\rangle e^{\frac{\mathbf{p}\cdot\mathbf{r}'}{i\hbar}} \left\langle \mathbf{r}+\frac{\mathbf{r}'}{2}\right| \ . \tag{39}$$

For any physical quantity a —described via the operator $\hat{a}$— its average value in (21) can be rewritten according to the Wigner picture just recalled as

$$\langle a\rangle = (2\pi\hbar)^{-3} \int d\mathbf{r}d\mathbf{p} a^{\rm W}(\mathbf{r},\mathbf{p}) f^{\rm W}(\mathbf{r},\mathbf{p}) \ , \tag{40}$$

where

$$a^{\rm W}(\mathbf{r},\mathbf{p}) = {\rm tr}\{\hat{W}(\mathbf{r},\mathbf{p})\hat{a}\} \tag{41}$$

is the Weyl-Wigner transform of the operator $\hat{a}$. Equation (40) is formally identical to its semiclassical counterpart in (14), thus confirming the central role played by the Wigner picture in establishing a direct link between the fully quantum-mechanical approach of Sec. III and the semiclassical theory of Sec. II (see below). However, apart from such formal similarity, the Wigner function in (38) is not positive-definite, and cannot be regarded as a classical phase-space distribution probability.[39,41]

The equation for the Wigner function in (38) can be derived from the equation of motion for the density-matrix operator in (22). More specifically, by applying the Weyl-Wigner transform (38), together with its inverse

$$\hat{\rho} = (2\pi\hbar)^{-3} \int d\mathbf{r} \int d\mathbf{p} \, \hat{W}(\mathbf{r},\mathbf{p}) \, f^{\rm W}(\mathbf{r},\mathbf{p}) \, , \tag{42}$$

to the density-matrix equation (22), one gets the equation of motion for the Wigner function:

$$\frac{\partial f^{\rm W}(\mathbf{r},\mathbf{p})}{\partial t} = \left.\frac{\partial f^{\rm W}(\mathbf{r},\mathbf{p})}{\partial t}\right|_{\rm sp} + \left.\frac{\partial f^{\rm W}(\mathbf{r},\mathbf{p})}{\partial t}\right|_{\rm scat} \tag{43}$$

with

$$\left.\frac{\partial f^{\rm W}(\mathbf{r},\mathbf{p})}{\partial t}\right|_{\rm sp} = \int d\mathbf{r}' \, d\mathbf{p}' \epsilon(\mathbf{r},\mathbf{p};\mathbf{r}',\mathbf{p}') f^{\rm W}(\mathbf{r}',\mathbf{p}') \tag{44}$$

and

$$\left.\frac{\partial f^{\rm W}(\mathbf{r},\mathbf{p})}{\partial t}\right|_{\rm scat} = \int d\mathbf{r}' \, d\mathbf{p}' \, \Gamma(\mathbf{r},\mathbf{p};\mathbf{r}',\mathbf{p}') f^{\rm W}(\mathbf{r}',\mathbf{p}') \ , \tag{45}$$

where

$$\epsilon(\mathbf{r},\mathbf{p};\mathbf{r}',\mathbf{p}') = -\frac{i}{(2\pi)^3\hbar^4} {\rm tr}\left\{\hat{W}(\mathbf{r},\mathbf{p}) \, \left[\hat{H}_{\rm sp}, \, \hat{W}(\mathbf{r}',\mathbf{p}')\right]\right\} \tag{46}$$

and

$$\Gamma(\mathbf{r},\mathbf{p};\mathbf{r}',\mathbf{p}') = (2\pi\hbar)^{-3} {\rm tr}\left\{\hat{W}(\mathbf{r},\mathbf{p}) \, \Gamma\left(\hat{W}(\mathbf{r}',\mathbf{p}')\right)\right\} \tag{47}$$

are the single-particle and the scattering superoperators written in the $(\mathbf{r},\mathbf{p})$ Wigner picture, respectively.

Denoting again with $|\alpha\rangle$ the eigenstates of $\hat{H}_{\rm sp}$ (see Eq. (26)), the Wigner function in (38) can be written as

$$f^{\rm W}(\mathbf{r},\mathbf{p}) = \sum_{\alpha_1\alpha_2} W_{\alpha_1\alpha_2}(\mathbf{r},\mathbf{p}) \rho_{\alpha_2\alpha_1} \tag{48}$$

where

$$W_{\alpha_1\alpha_2}(\mathbf{r},\mathbf{p}) = \int d\mathbf{r}' \phi^*_{\alpha_1}\left(\mathbf{r}-\frac{\mathbf{r}'}{2}\right) e^{\frac{\mathbf{p}\cdot\mathbf{r}'}{i\hbar}} \phi_{\alpha_2}\left(\mathbf{r}+\frac{\mathbf{r}'}{2}\right) \tag{49}$$

are the matrix elements of the Wigner operator in (39).

B. Quantum nonlocality

We shall now show that, opposite to the semiclassical equation in (11), the Wigner transport equation (43) may be non-local both in $\mathbf{r}$ and in $\mathbf{p}$. To this end, we shall investigate the explicit form of the single-particle and scattering superoperators in (46) and (47) corresponding to a realistic description of the quantum nanomaterial under examination.

In order to evaluate the peculiar features of the single-particle superoperator in (46), we shall adopt an envelope-function Hamiltonian[7] of the form[57]

$$\hat{H}_{\rm sp} = K(\hat{\mathbf{p}}) + V(\hat{\mathbf{r}}) \ , \tag{50}$$

where $\hat{\mathbf{r}}$ and $\hat{\mathbf{p}}$ denote, respectively, the quantum-mechanical operators associated to the electronic coordinate ($\mathbf{r}$) and momentum ($\mathbf{p}$). According to the usual prescription of the envelope-function theory, the function K in Eq. (50) describes the bulk electronic band, while V describes the nanostructure potential profile. By inserting the envelope-function Hamiltonian (50) into Eq. (46), after a straightforward calculation (not reported here), one gets

$$\left.\frac{\partial f^{\rm W}(\mathbf{r},\mathbf{p})}{\partial t}\right|_{\rm sp} = \left.\frac{\partial f^{\rm W}(\mathbf{r},\mathbf{p})}{\partial t}\right|_{K} + \left.\frac{\partial f^{\rm W}(\mathbf{r},\mathbf{p})}{\partial t}\right|_{V} \ , \tag{51}$$

where

$$\left.\frac{\partial f(\mathbf{r},\mathbf{p})}{\partial t}\right|_{K} = -\int d\mathbf{r}' \mathcal{K}(\mathbf{r}-\mathbf{r}',\mathbf{p}) f^{\rm W}(\mathbf{r}',\mathbf{p}) \tag{52}$$

with

$$\mathcal{K}(\mathbf{r}'',\mathbf{p}) = i\int d\mathbf{p}' \frac{e^{-\frac{\mathbf{r}''\cdot\mathbf{p}'}{i\hbar}}}{(2\pi)^3\hbar^4}\left[K\left(\mathbf{p}+\frac{\mathbf{p}'}{2}\right) - K\left(\mathbf{p}-\frac{\mathbf{p}'}{2}\right)\right] \ , \tag{53}$$

and

$$\left.\frac{\partial f(\mathbf{r},\mathbf{p})}{\partial t}\right|_{V} = -\int d\mathbf{p}' \mathcal{V}(\mathbf{r},\mathbf{p}-\mathbf{p}') f^{\rm W}(\mathbf{r},\mathbf{p}') \tag{54}$$

with

$$\mathcal{V}(\mathbf{r},\mathbf{p}'') = i\int d\mathbf{r}' \frac{e^{\frac{\mathbf{p}''\cdot\mathbf{r}'}{i\hbar}}}{(2\pi)^3\hbar^4}\left[V\left(\mathbf{r}+\frac{\mathbf{r}'}{2}\right) - V\left(\mathbf{r}-\frac{\mathbf{r}'}{2}\right)\right] \ . \tag{55}$$

As we can see, the kinetic superoperator $\mathcal{K}$ in (52) is always local in $\mathbf{p}$ and, in general, is non-local in $\mathbf{r}$. In particular, by adopting the usual effective-mass approximation,

$$K(\mathbf{p}) = \frac{p^2}{2m^*} \ , \tag{56}$$

the non-local kinetic operator (52) reduces to

$$\left.\frac{\partial f^{\rm W}(\mathbf{r},\mathbf{p})}{\partial t}\right|_{K} = -\mathbf{v}(\mathbf{p})\cdot\frac{\partial f^{\rm W}(\mathbf{r},\mathbf{p})}{\partial \mathbf{r}} \ , \tag{57}$$

where $\mathbf{v}(\mathbf{p})$ denotes the carrier group velocity of the semiclassical theory (see Eq. (5)). Notably, within the effective-mass approximation (56) the kinetic contribution coincides with its semiclassical counterpart, i.e., it reduces to the standard diffusion term of the Boltzmann equation (see Eq. (7)).

Oppositely to the kinetic one, the potential superoperator $\mathcal{V}$ in (54) is always local in $\mathbf{r}$ and, in general, is non-local in $\mathbf{p}$. For the particular case of a quadratic potential

$$V(\mathbf{r}) = \frac{1}{2}ar^2 + \mathbf{b}\cdot\mathbf{r} \quad , \tag{58}$$

corresponding to the classical force

$$\mathbf{F}(\mathbf{r}) = -\frac{\partial V}{\partial \mathbf{r}} = -(a\mathbf{r}+\mathbf{b}), \tag{59}$$

the non-local potential superoperator (54) simply reduces to

$$\left.\frac{\partial f^{\rm W}(\mathbf{r},\mathbf{p})}{\partial t}\right|_{V} = -\mathbf{F}(\mathbf{r})\cdot\frac{\partial f^{\rm W}(\mathbf{r},\mathbf{p})}{\partial \mathbf{p}} \ . \tag{60}$$

Thus, for the particular case of the quadratic potential profile in (58), the potential contribution coincides with its semiclassical counterpart, i.e., it reduces to the standard drift term of the Boltzmann equation (see Eq. (7)); it follows that the non-local character of the generic potential superoperator in (54) vanishes in the presence of a parabolic potential only.

At this point a few comments are in order. The analysis performed so far has shown that within the Wigner picture real-space ($\mathbf{r}$) and momentum ($\mathbf{p}$) coordinates play a strongly symmetric role. Moreover, for a physical system characterized by an effective Hamiltonian quadratic in both the coordinate and the momentum, the equation of motion of the Wigner function coincides with its semiclassical (Boltzmann) counterpart, thus showing once again the intimate link between the Wigner function and the semiclassical carrier distribution. This can also be regarded as a formal proof of the fact that, for a particle subjected to a quadratic potential, its classical and quantum equations of motion coincide, a fundamental result originally pointed out by Richard P. Feynman via his "path integral" formulation of quantum mechanics.[58]

Let us now discuss the general non-local features of the scattering superoperator in (47). By inserting into Eq. (47) the explicit form of the Lindblad-like superoperator (25), we get:

$$\Gamma(\mathbf{r},\mathbf{p};\mathbf{r}',\mathbf{p}') = (2\pi\hbar)^{-3}\sum_s \Re\left\{\mathrm{tr}\left\{\hat{W}(\mathbf{r},\mathbf{p})\,\hat{A}^s\hat{W}(\mathbf{r}',\mathbf{p}')\hat{A}^{\dagger s}\right\} - \mathrm{tr}\left\{\hat{W}(\mathbf{r},\mathbf{p})\,\hat{A}^{s\dagger}\hat{A}^s\hat{W}(\mathbf{r}',\mathbf{p}')\right\}\right\} \ . \tag{61}$$

As shown in the following section, in the so-called semiclassical limit these two contributions reduce to the in- and out-scattering terms of the Boltzmann theory; however, opposite to the Boltzmann collision term in Eq. (8), the quantum-mechanical scattering superoperator in (61) is in general spatially non-local. Indeed, for a generic Lindblad operator $\hat{A}^s$ corresponding to a given interaction mechanism s, the scattering superoperator is in general different from zero also for $\mathbf{r} \neq \mathbf{r}'$.

In order to better elucidate the spatial nonlocality of the Wigner-transport theory, it is useful to recall the link between our Wigner function $f^{\rm W}(\mathbf{r},\mathbf{p})$ and the corresponding spatial carrier density $n(\mathbf{r})$; according to the general average-value prescription (40), one gets a result formally identical to the semiclassical one in (15):

$$n(\mathbf{r}) = (2\pi\hbar)^{-3} \int d^3p\, f^{\rm W}(\mathbf{r},\mathbf{p}) \ . \tag{62}$$

Combining the above result with the Wigner transport equation (43) and employing the single-particle results in (51)-(55), the time evolution of the spatial carrier density is again given by Eq. (16) with

$$\left.\frac{\partial n(\mathbf{r})}{\partial t}\right|_{\rm sp} = -(2\pi\hbar)^{-3} \int d\mathbf{r}' d\mathbf{p}' \mathcal{K}(\mathbf{r}-\mathbf{r}',\mathbf{p}') f^{\rm W}(\mathbf{r}',\mathbf{p}') \tag{63}$$

and

$$\left.\frac{\partial n(\mathbf{r})}{\partial t}\right|_{\rm scat} = (2\pi\hbar)^{-3} \int d\mathbf{r}' d\mathbf{p} d\mathbf{p}' \Gamma(\mathbf{r},\mathbf{p};\mathbf{r}',\mathbf{p}') f^{\rm W}(\mathbf{r}',\mathbf{p}') \ . \tag{64}$$

It is important to stress that, also within the present quantum-mechanical treatment, the time evolution of the spatial carrier density in Eq. (16) can be expressed via the usual charge continuity equation in (20). To this end, the carrier current density $\mathbf{J}(\mathbf{r})$ is defined as the average value (see Eqs. (40) and (41)) of a corresponding quantum-mechanical operator $\hat{\mathbf{J}}(\mathbf{r})$ as

$$\mathbf{J}(\mathbf{r}) = (2\pi\hbar)^{-3} \int d\mathbf{r}' d\mathbf{p}' \mathbf{J}^{\rm W}(\mathbf{r};\mathbf{r}',\mathbf{p}') f^{\rm W}(\mathbf{r}',\mathbf{p}') \ , \tag{65}$$

where

$$\mathbf{J}^{\rm W}(\mathbf{r};\mathbf{r}',\mathbf{p}') = {\rm tr}\{\hat{W}(\mathbf{r}',\mathbf{p}')\hat{\mathbf{J}}(\mathbf{r})\} \tag{66}$$

is the Weyl-Wigner transform of the current-density operator. Combining Eqs. (16), (20), (63), and (64), after a straightforward calculation (not reported here) one gets

$$\mathbf{J}^{\rm W}(\mathbf{r};\mathbf{r}',\mathbf{p}') = \mathbf{J}^{\rm W}_{\rm sp}(\mathbf{r};\mathbf{r}',\mathbf{p}') + \mathbf{J}^{\rm W}_{\rm scat}(\mathbf{r};\mathbf{r}',\mathbf{p}') \tag{67}$$

with

$$\mathbf{J}^{\rm W}_{\rm sp}(\mathbf{r};\mathbf{r}',\mathbf{p}') = (2\pi\hbar)^{-3} \int d\mathbf{r}'' d\mathbf{p}'' \frac{e^{\frac{\mathbf{p}''\cdot(\mathbf{r}''-\mathbf{r})}{i\hbar}}}{i\mathbf{p}''} \mathcal{K}(\mathbf{r}''-\mathbf{r}',\mathbf{p}') \tag{68}$$

and

$$\mathbf{J}^{\rm W}_{\rm scat}(\mathbf{r};\mathbf{r}',\mathbf{p}') = -(2\pi\hbar)^{-3} \int d\mathbf{r}'' d\mathbf{p} d\mathbf{p}'' \frac{e^{\frac{\mathbf{p}''\cdot(\mathbf{r}''-\mathbf{r})}{i\hbar}}}{i\mathbf{p}''} \Gamma(\mathbf{r}'',\mathbf{p};\mathbf{r}',\mathbf{p}') \ . \tag{69}$$

It follows that the quantum-mechanical current density in (65) is the sum of a single-particle and of a scattering contribution; it is worth stressing that the presence of a scattering-induced current has been clearly pointed out by Gebauer and Car in Ref. 59.

While for the particular case of a parabolic band the kinetic term of the Wigner equation reduces to the diffusion term of the Boltzmann theory and the single-particle current is simply given by the Wigner-picture version of Eq. (18), i.e.,

$$\mathbf{J}_{\rm sp}(\mathbf{r}) = (2\pi\hbar)^{-3} \int d^3p\, \mathbf{v}(\mathbf{p})\, f^{\rm W}(\mathbf{r},\mathbf{p}) \ , \tag{70}$$

for non-parabolic bands the single-particle current density is always described in terms of the spatially non-local superoperator in (68).[51–53]

The explicit form of the scattering-induced current-density operator in (69) will depend strongly on the specific form of the scattering superoperator Γ. In any case, opposite to the semiclassical scenario, within a fully quantum-mechanical description such scattering-induced current is in general different from zero, which is again a clear fingerprint of the non-local character of our scattering superoperator.

C. The semiclassical limit

In what follows we shall discuss the so-called semiclassical limit, namely we shall recover the Boltzmann transport theory of Sec. II as the limit of the previous Wigner transport theory for $\hbar \to 0$.

As far as the single-particle contribution in (51) is concerned, it is useful to recall that the latter may be conveniently expressed via the so-called Moyal brackets,[60] a quantum-mechanical generalization[41] of the classical Poisson brackets in (13). More specifically, it is possible

to show that

$$\left.\frac{\partial f^{\mathrm{W}}}{\partial t}\right|_{\mathrm{sp}} = -\left\{f^{\mathrm{W}}, H_{\mathrm{sp}}\right\}_{\mathrm{M}} \ , \tag{71}$$

where

$$\{a,b\}_{\mathrm{M}} = \frac{2}{\hbar}\sin\left[\frac{\hbar}{2}\left(\frac{\partial}{\partial \mathbf{r}}\frac{\partial}{\partial \mathbf{p}'} - \frac{\partial}{\partial \mathbf{p}}\frac{\partial}{\partial \mathbf{r}'}\right)\right] a(\mathbf{r},\mathbf{p})b(\mathbf{r}',\mathbf{p}')\Big|_{\mathbf{r},\mathbf{p}=\mathbf{r}',\mathbf{p}'} \tag{72}$$

denotes the Moyal brackets applied to two generic phase-space functions a and b.

By expanding the sine function with respect to its argument, it is easy to write the above single-particle contribution as a series expansion in powers of $\hbar$; moreover, the lowest-order contribution is $\hbar$-independent and coincides with the Poisson brackets in (13). As a result we get

$$\left.\frac{\partial f^{\mathrm{W}}}{\partial t}\right|_{\mathrm{sp}} = -\left\{f^{\mathrm{W}}, H_{\mathrm{sp}}\right\}_{\mathrm{P}} + o\left(\hbar^2\right) \ , \tag{73}$$

which shows that —as expected— in the semiclassical limit ($\hbar \to 0$) the quantum-mechanical (Wigner) single-particle contribution reduces to its classical (Boltzmann) counterpart in (12).

As discussed previously, for a physical system characterized by an effective Hamiltonian quadratic in both the coordinate and the momentum, its quantum and classical scattering-free dynamics coincide; this can be easily understood in terms of the present Moyal formalism, noticing that in this particular case all higher-order contributions in the power expansion are always equal to zero, regardless of the value of $\hbar$. It follows that, while for a quadratic Hamiltonian the quantum single-particle dynamics is always local, for a generic band structure as well as for a generic potential profile the latter is intrinsically non-local, and becomes local only in the semiclassical limit $\hbar \to 0$.

Let us now face the most difficult task of the semiclassical limit, showing that for $\hbar \to 0$ the fully quantum-mechanical scattering dynamics in (45) reduces to the standard collision term of the Boltzmann theory in (8). To this aim, the first step is to rewrite the Lindblad-like scattering superoperator in (61) within the momentum representation. More specifically, taking into account that

$$\langle \mathbf{p}_1|\hat{W}(\mathbf{r},\mathbf{p})|\mathbf{p}_2\rangle = e^{\frac{(\mathbf{p}_1-\mathbf{p}_2)\cdot\mathbf{r}}{i\hbar}}\delta\left(\frac{\mathbf{p}_1+\mathbf{p}_2}{2}-\mathbf{p}\right) \ , \tag{74}$$

the explicit form of the scattering superoperator in (61) comes out to be

$$\begin{aligned}\Gamma(\mathbf{r},\mathbf{p};\mathbf{r}',\mathbf{p}') = &\left(\frac{2}{\pi\hbar}\right)^3 \sum_s \int d\mathbf{p}_1 d\mathbf{p}_2 e^{\frac{2(\mathbf{p}_1-\mathbf{p}_2+\mathbf{p}'-\mathbf{p})\cdot\mathbf{r}}{i\hbar}} A^s(2\mathbf{p}-\mathbf{p}_1, 2\mathbf{p}'-\mathbf{p}_2)A^{s*}(\mathbf{p}_1,\mathbf{p}_2)e^{-\frac{2(\mathbf{p}_2-\mathbf{p}')\cdot(\mathbf{r}'-\mathbf{r})}{i\hbar}} \\ &- \left(\frac{2}{\pi\hbar}\right)^3 \sum_s \Re\left\{\int d\mathbf{p}_1 d\mathbf{p}_2 e^{\frac{2(\mathbf{p}'-\mathbf{p})\cdot\mathbf{r}}{i\hbar}} A^{s*}(\mathbf{p}_2, 2\mathbf{p}-\mathbf{p}_1)A^s(\mathbf{p}_2, 2\mathbf{p}'-\mathbf{p}_1)e^{-\frac{2(\mathbf{p}_1-\mathbf{p}')\cdot(\mathbf{r}'-\mathbf{r})}{i\hbar}}\right\} \ . \end{aligned} \tag{75}$$

By inserting the above result into Eq. (45), one gets:

$$\begin{aligned}\left.\frac{\partial f^{\mathrm{W}}(\mathbf{r},\mathbf{p})}{\partial t}\right|_{\mathrm{scat}} = &\left(\frac{2}{\pi\hbar}\right)^3 \sum_s \int d\mathbf{r}' d\mathbf{p}' d\mathbf{p}_1 d\mathbf{p}_2 e^{\frac{2(\mathbf{p}_1-\mathbf{p}_2+\mathbf{p}'-\mathbf{p})\cdot\mathbf{r}}{i\hbar}} A^s(2\mathbf{p}-\mathbf{p}_1, 2\mathbf{p}'-\mathbf{p}_2)A^{s*}(\mathbf{p}_1,\mathbf{p}_2)e^{-\frac{2(\mathbf{p}_2-\mathbf{p}')\cdot(\mathbf{r}'-\mathbf{r})}{i\hbar}} f^{\mathrm{W}}(\mathbf{r}',\mathbf{p}') \\ &- \left(\frac{2}{\pi\hbar}\right)^3 \sum_s \Re\left\{\int d\mathbf{r}' d\mathbf{p}' d\mathbf{p}_1 d\mathbf{p}_2 e^{\frac{2(\mathbf{p}'-\mathbf{p})\cdot\mathbf{r}}{i\hbar}} A^{s*}(\mathbf{p}_2, 2\mathbf{p}-\mathbf{p}_1)A^s(\mathbf{p}_2, 2\mathbf{p}'-\mathbf{p}_1)e^{-\frac{2(\mathbf{p}_1-\mathbf{p}')\cdot(\mathbf{r}'-\mathbf{r})}{i\hbar}} f^{\mathrm{W}}(\mathbf{r}',\mathbf{p}')\right\} \end{aligned} \tag{76}$$

.

Let us now analyze the semiclassical limit of the above quantum-mechanical scattering superoperator. From a

physical point of view, in the limit $\hbar \to 0$ the various phase factors entering Eq. (76) will display infinitely fast oscillations, which allows one to evaluate some of the above coordinate and momentum integrals via a sort of adiabatic-decoupling procedure. As far as the coordinate $\mathbf{r}'$ is concerned, for any regular function $F(\mathbf{r})$ we have:

$$\lim_{\hbar\to 0}\int d\mathbf{r}' e^{\frac{\mathbf{p}''\cdot(\mathbf{r}'-\mathbf{r})}{i\hbar}} F(\mathbf{r}') = (2\pi\hbar)^3\delta(\mathbf{p}'')F(\mathbf{r}) \ . \quad (77)$$

By employing this general property, in the semiclassical limit ($\hbar \to 0$) the scattering superoperator in (76) simplifies to:

$$\left.\frac{\partial f^{\mathrm{W}}(\mathbf{r},\mathbf{p})}{\partial t}\right|_{\mathrm{scat}} = 8\sum_s \int d\mathbf{p}' d\mathbf{p}_1 e^{\frac{2(\mathbf{p}_1-\mathbf{p})\cdot\mathbf{r}}{i\hbar}} A^s(2\mathbf{p}-\mathbf{p}_1,\mathbf{p}') A^{s*}(\mathbf{p}_1,\mathbf{p}') f^{\mathrm{W}}(\mathbf{r},\mathbf{p}')$$
$$- 8\sum_s \Re\left\{\int d\mathbf{p}' d\mathbf{p}_2 e^{\frac{2(\mathbf{p}'-\mathbf{p})\cdot\mathbf{r}}{i\hbar}} A^{s*}(\mathbf{p}_2,2\mathbf{p}-\mathbf{p}') A^s(\mathbf{p}_2,\mathbf{p}') f^{\mathrm{W}}(\mathbf{r},\mathbf{p}')\right\} \ . \quad (78)$$

In addition to the spatial adiabatic decoupling in (77), in the semiclassical limit it is also possible to show that for any regular function $G(\mathbf{r},\mathbf{p})$:

$$\lim_{\hbar\to 0}\int d\mathbf{p}'' e^{\frac{(\mathbf{p}''-\mathbf{p})\cdot\mathbf{r}}{i\hbar}} G(\mathbf{r},\mathbf{p}'') = \frac{(2\pi\hbar)^3}{\Omega} G(\mathbf{r},\mathbf{p}) \ . \quad (79)$$

Here Ω is the very same crystal normalization volume introduced in Eq. (10); indeed, in order to derive this result it is crucial to perform a sort of spatial coarse graining, i.e., a spatial average of the function G over a volume Ω much larger than the typical carrier coherence length and much smaller than the macroscopic spatial variations of our material. By employing the general property in (79) the scattering superoperator in (78) reduces to:

$$\left.\frac{\partial f^{\mathrm{W}}(\mathbf{r},\mathbf{p})}{\partial t}\right|_{\mathrm{scat}} = \frac{(2\pi\hbar)^3}{\Omega}\sum_s \int d\mathbf{p}' \left[|A^s(\mathbf{p},\mathbf{p}')|^2 f^{\mathrm{W}}(\mathbf{r},\mathbf{p}') - |A^s(\mathbf{p}',\mathbf{p})|^2 f^{\mathrm{W}}(\mathbf{r},\mathbf{p})\right] \ . \quad (80)$$

This is exactly the Boltzmann collision term of the semiclassical theory we were looking for; indeed, the latter can be written in a more compact form as

$$\left.\frac{\partial f^{\mathrm{W}}}{\partial t}\right|_{\mathrm{scat}} = \int d^3p' \left[P(\mathbf{p},\mathbf{p}')f^{\mathrm{W}}(\mathbf{r},\mathbf{p}') - P(\mathbf{p}',\mathbf{p})f^{\mathrm{W}}(\mathbf{r},\mathbf{p})\right] \ , \quad (81)$$

where $P(\mathbf{p},\mathbf{p}')$ can be written again according to Eq. (9) as the sum of scattering rates

$$P^s(\mathbf{p},\mathbf{p}') = \frac{(2\pi\hbar)^3}{\Omega}|A^s(\mathbf{p},\mathbf{p}')|^2 \quad (82)$$

corresponding to the various interaction mechanisms s.

Equation (81) is formally identical to the Boltzmann collision term in (8), thus showing that in the semiclassical limit the fully quantum-mechanical scattering superoperator of the Wigner theory reduces to the Boltzmann one. Moreover, the semiclassical-limit procedure presented so far shows that the scattering rates of the Boltzmann transport theory can be easily expressed in terms of the matrix elements $A^s(\mathbf{p},\mathbf{p}')$ of the various Lindblad operators (see Eq. (82)). As already discussed in Sec. II, in order to establish a direct link with the conventional Fermi's-golden-rule prescription, it is convenient to move from the continuous momentum representation employed so far to its discrete version corresponding to the crystal normalization volume Ω; more precisely, employing the continuous-versus-discrete prescription in (10)), the scattering rates in (82) can also be written as

$$P^s_{\mathbf{p},\mathbf{p}'} = \left|A^s_{\mathbf{p},\mathbf{p}'}\right|^2 \ , \quad (83)$$

in total agreement with the diagonal-approximation result in (36).

V. SCATTERING-INDUCED DIFFUSION: A FEW SIMULATED EXPERIMENTS

Aim of this section is to perform a detailed investigation of scattering-induced diffusion in state-of-the-art semiconductor bulk and nanostructures. Based on the quantum-transport formulation proposed so far, we shall present and discuss a number of simulated experiments of ultrafast carrier dynamics in GaN-based materials.

A. Physical model and simulation strategy

As physical system we shall consider an effective one-dimensional GaN-based nanostructure, whose main energy-dissipation/decoherence mechanism is carrier-LO phonon scattering. In order to mimic the main features of a realistic GaN-based material, the following parameters have been employed: effective mass $m^* = 0.2m_\circ$ ($m_\circ$ denoting the free-electron one), LO-phonon energy $\epsilon_{\rm LO} = 80\,{\rm meV}$, and average bulk carrier-LO phonon scattering rate $\tau_{\rm LO} = 25\,{\rm fs}$.

For the case of a one-dimensional system with coordinate z and momentum p, the space (see Eq. (31)) and momentum charge distributions are simply given by

$$n(z) = \sum_{\alpha_1\alpha_2} \phi_{\alpha_1}(z)\rho_{\alpha_1\alpha_2}\phi^*_{\alpha_2}(z) \tag{84}$$

and

$$n(p) = \sum_{\alpha_1\alpha_2} \tilde{\phi}_{\alpha_1}(p)\rho_{\alpha_1\alpha_2}\tilde{\phi}^*_{\alpha_2}(p)\ , \tag{85}$$

where $\phi_\alpha(z) \equiv \langle z|\alpha\rangle$ denotes the real-space wavefunction corresponding to the eigenstate α, and $\tilde{\phi}_\alpha(p) \equiv \langle p|\alpha\rangle$ its Fourier transform.

Combining the prescription in (84) with the density-matrix equation (28), the total time evolution of the spatial carrier density can be written as the one-dimensional version of Eq. (16), namely

$$\frac{\partial n(z)}{\partial t} = \left.\frac{\partial n(z)}{\partial t}\right|_{\rm sp} + \left.\frac{\partial n(z)}{\partial t}\right|_{\rm scat} \tag{86}$$

with

$$\left.\frac{\partial n(z)}{\partial t}\right|_{\rm sp} = \sum_{\alpha_1\alpha_2} \phi_{\alpha_1}(z)\frac{\epsilon_{\alpha_1}-\epsilon_{\alpha_2}}{i\hbar}\rho_{\alpha_1\alpha_2}\phi^*_{\alpha_2}(z) \tag{87}$$

and

$$\left.\frac{\partial n(z)}{\partial t}\right|_{\rm scat} = \sum_{\alpha_1\alpha_2} \phi_{\alpha_1}(z)\left.\frac{d\rho_{\alpha_1\alpha_2}}{dt}\right|_{\rm scat}\phi^*_{\alpha_2}(z)\ . \tag{88}$$

As already pointed out in Secs. IV B and IV C, for the relevant case of the Lindblad superoperator in (29) the corresponding time evolution can be expressed as the difference of two terms, which in the semiclassical limit reduce to the in- minus out-scattering structure of the conventional Boltzmann theory (see Eq. (8)). This suggests to rewrite the scattering superoperator in (29) as:

$$\left.\frac{d\rho_{\alpha_1\alpha_2}}{dt}\right|_{\rm scat} = F^{\rm in}_{\alpha_1\alpha_2} - F^{\rm out}_{\alpha_1\alpha_2} \tag{89}$$

with

$$F^{\rm in}_{\alpha_1\alpha_2} = \sum_{\alpha'_1\alpha'_2} \mathcal{P}_{\alpha_1\alpha_2,\alpha'_1\alpha'_2}\rho_{\alpha'_1\alpha'_2} \tag{90}$$

and

$$F^{\rm out}_{\alpha_1\alpha_2} = \frac{1}{2}\sum_{\alpha'_1\alpha'_2} \mathcal{P}^*_{\alpha'_1\alpha'_1,\alpha_1\alpha'_2}\rho_{\alpha'_2\alpha_2} + {\rm H.c.}\ . \tag{91}$$

By inserting Eq. (89) into Eq. (88), one gets:

$$\left.\frac{\partial n(z)}{\partial t}\right|_{\rm scat} = F^{\rm in}(z) - F^{\rm out}(z) \tag{92}$$

with

$$F^{\rm in/out}(z) = \sum_{\alpha_1\alpha_2} \phi_{\alpha_1}(z)F^{\rm in/out}_{\alpha_1\alpha_2}\phi^*_{\alpha_2}(z)\ . \tag{93}$$

It is easy to show that the in-scattering contribution $F^{\rm in}_{\alpha_1\alpha_2}$ in (90) (corresponding to the first term of the Lindblad superoperator in (25)) is always positive-definite; this implies that the corresponding charge-density variation $F^{\rm in}(z)$ is always positive-definite as well. We stress that this does not apply to the out-scattering contribution $F^{\rm out}(z)$.

Our simulation strategy is based on a numerical solution of the density-matrix equation in (28); this is realized via a fixed-time-step discretization[20] based on an exact integration of the single-particle dynamics. More specifically, the single-particle states α of the structure under examination are described via the standard envelope-function and effective-mass approximations (see Eqs. (50) and (56))[7] in terms of a plane-wave expansion.[20]

For all the simulated experiments presented below we have chosen as initial condition a single-particle density matrix $\overline{\rho}_{\alpha_1\alpha_2}$ corresponding to a gaussian carrier distribution both in space and momentum, namely

$$\overline{n}(z) \propto \frac{e^{-\frac{z^2}{2\overline{\Delta}_z^2}}}{\sqrt{2\pi}\,\overline{\Delta}_z}\ , \qquad \overline{n}(p) \propto \frac{e^{-\frac{p^2}{2\overline{\Delta}_p^2}}}{\sqrt{2\pi}\,\overline{\Delta}_p}\ , \tag{94}$$

where $\overline{\Delta}_z$ describes the degree of spatial localization of our initial state, and $\overline{\Delta}_p = \sqrt{m^* k_B T}$ describes the thermal fluctuations of our carrier gas.

It is easy to show that such initial condition corresponds to a Wigner function

$$\overline{f}^{\rm W}(z,p) \propto \hbar\,\frac{e^{-\frac{z^2}{2\overline{\Delta}_z^2}}e^{-\frac{p^2}{2\overline{\Delta}_p^2}}}{\sqrt{2\pi}\,\overline{\Delta}_z\overline{\Delta}_p}\ , \tag{95}$$

and therefore to an initial density matrix

$$\overline{\rho}_{\alpha_1\alpha_2} \propto \frac{1}{2\pi}\int dz\,dp W_{\alpha_1\alpha_2}(z,p)\frac{e^{-\frac{z^2}{2\overline{\Delta}_z^2}}e^{-\frac{p^2}{2\overline{\Delta}_p^2}}}{\sqrt{2\pi}\,\overline{\Delta}_z\overline{\Delta}_p}\ , \tag{96}$$

where

$$W_{\alpha_1\alpha_2}(z,p) = \int dz'\phi^*_{\alpha_1}\left(z-\frac{z'}{2}\right)e^{\frac{pz'}{i\hbar}}\phi_{\alpha_2}\left(z+\frac{z'}{2}\right) \tag{97}$$

is the one-dimensional version of the Weyl-Wigner transform in (49).

The (mixed-state) density matrix in (96) is not always physical; indeed, it is possible to show that the uncertainty principle imposes the following restriction: $\overline{\Delta}_z \geq \frac{\hbar}{2\overline{\Delta}_p}$. Recalling that $\overline{\Delta}_p = \sqrt{m^* k_B T}$, it follows that at room temperature and for the GaN parameters previously recalled, one gets: $\overline{\Delta}_z \geq \frac{\hbar}{2\sqrt{m^* k_B T}} \simeq 2\,\text{nm}$.

Primary goal of our simulated experiments is to investigate the non-local character of the Lindblad-like scattering superoperator in (29), and to compare it with other scattering models. The simplest parameter-free form of the scattering term entering our density-matrix equation (28) is given by the following relaxation-time model:[61]

$$\left.\frac{d\rho_{\alpha_1\alpha_2}}{dt}\right|_{\text{scat}} = -\frac{\Gamma_{\alpha_1}+\Gamma_{\alpha_2}}{2}\left(\rho_{\alpha_1\alpha_2}-\rho^{\circ}_{\alpha_1\alpha_2}\right) \ . \qquad (98)$$

Here $\rho^{\circ}_{\alpha_1\alpha_2} = f^{\circ}_{\alpha_1}\delta_{\alpha_1\alpha_2}$ is the equilibrium density matrix dictated by the host material, and

$$\Gamma_{\alpha} = \sum_{s}\sum_{\alpha'} P^{s}_{\alpha'\alpha} \qquad (99)$$

is the total scattering rate (i.e., summed over all final states α' and relevant interaction mechanisms s) corresponding to the microscopic transition probabilities $P^{s}_{\alpha'\alpha}$ of the semiclassical transport theory given by the standard Fermi's golden rule.[8] Within such relaxation-time paradigm, the diagonal contributions ($\alpha_1 = \alpha_2$) describe population transfer (and thus energy dissipation) toward the equilibrium carrier distribution $f^{\circ}_{\alpha_1}$ according to the relaxation rate Γ_{α_1}, whereas the off-diagonal contributions ($\alpha_1 \neq \alpha_2$) describe a decay of the inter-state polarizations according to the decoherence/dephasing rate $(\Gamma_{\alpha_1}+\Gamma_{\alpha_2})/2$.

In spite of its simple form and straightforward physical interpretation, the structure of the relaxation-time term (98) is intrinsically different from the in- minus out-structure of the Boltzmann collision term as well as of the Lindblad superoperator in (29), and for this reason it may lead to a significant overestimation of decoherence processes (see below).

B. Analysis of bulk systems

Our first set of room-temperature simulated experiments corresponds to a GaN bulk system (i.e., no confinement potential profile).

1. *Scattering nonlocality*

Let us start our analysis by investigating the carrier-LO phonon scattering nonlocality induced by the Lindblad superoperator in (89). Figure 1 shows the initial time derivative of the spatial carrier density (see Eq. (88))

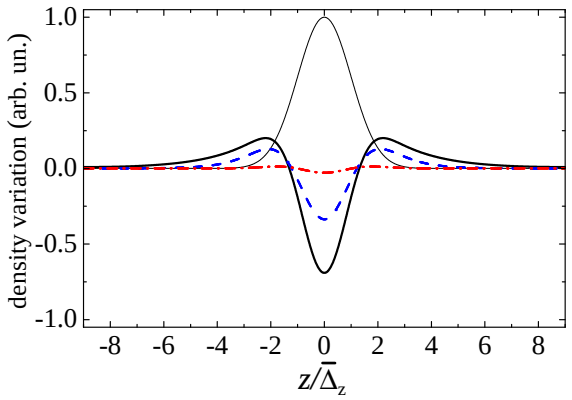

FIG. 1. (Color online) Carrier-LO phonon scattering nonlocality induced by the Lindblad superoperator in Eq. (89) in a GaN bulk system: initial time derivative of the spatial carrier density (see Eq. (88)) as a function of the relative coordinate $z/\overline{\Delta}_z$ for three different values of the localization parameter: $\overline{\Delta}_z = 5\,\text{nm}$ (solid curve), $\overline{\Delta}_z = 10\,\text{nm}$ (dashed curve), and $\overline{\Delta}_z = 50\,\text{nm}$ (dash-dotted curve), together with the initial spatial density profile in Eq. (94) (thin solid curve) (see text).

as a function of the relative coordinate $z/\overline{\Delta}_z$ for three different values of the localization parameter $\overline{\Delta}_z$. As we can see, in the presence of an initial nanometric confinement (solid and dashed curves) the phonon-induced time variation is significantly different from zero; the latter displays a negative peak —corresponding to a sort of replica of the initial distribution— and, more importantly, a positive contribution extending over a much larger range. This is exactly the signature of scattering-induced spatial nonlocality we were looking for. By significantly increasing the value of $\overline{\Delta}_z$ (dash-dotted curve), the magnitude and relative spatial extension of such nonlocality effects is strongly reduced, thus confirming that in the semiclassical limit $\overline{\Delta}_z \to \infty$ the scattering-induced time variation tends to zero, as predicted by the conventional Boltzmann theory (see Eq. (19)).

In order to better understand the physical origin and relative magnitude of the positive versus negative regions in Fig. 1, let us examine separately the impact of in- and out-scattering terms (see Eqs. (92) and (93)). Figure 2 shows in- (panel a) and out-scattering contributions (panel b) corresponding to the initial time derivatives of the spatial carrier density (see Eq. (92)) reported in Fig. 1. As we can see, in the presence of an initial nanometric confinement (solid and dashed curves) the in-scattering contribution (panel a) is significantly larger than the initial distribution profile (see thin solid curve in Fig. 1) while, in contrast, the out-scattering contribution (panel b) comes out to be more localized. It is exactly such different spatial extension of in- and out-scattering contributions that gives rise to the density-variation profiles in Fig. 1; in particular, the significant delocalization of the in-scattering contribution (compared to the out-scattering one) is responsible (i) of the negative cen-

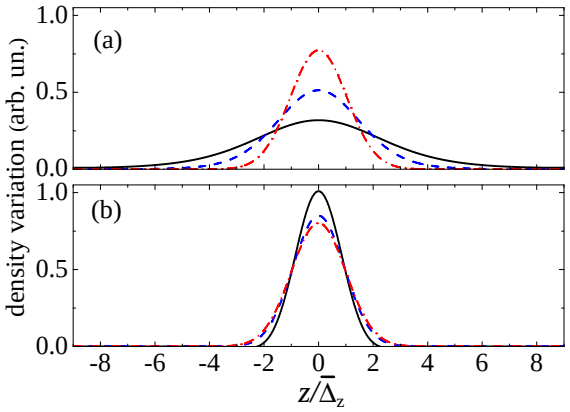

FIG. 2. (Color online) Carrier-LO phonon scattering nonlocality induced by the Lindblad superoperator in Eq. (89) in a GaN bulk system: in- (panel a) and out-scattering contributions (panel b) corresponding to the initial time derivatives of the spatial carrier density (see Eq. (92)) reported in Fig. 1 (see text).

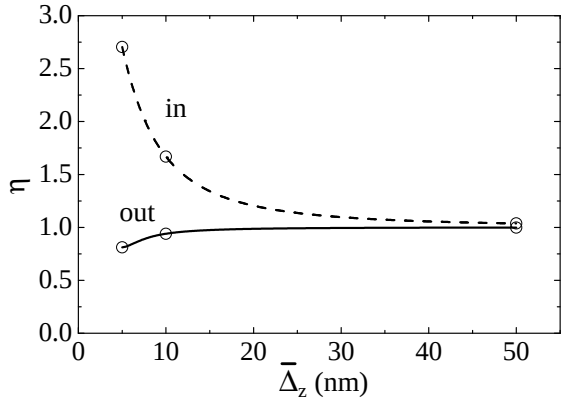

FIG. 3. (Color online) Nonlocality parameter in Eq. (100) as a function of $\overline{\Delta}_z$ for both in- and out-scattering contributions. Here, the 5 nm, 10 nm, and 50 nm values (see symbols) correspond to the in- and out-scattering profiles of Fig. 2 (see text).

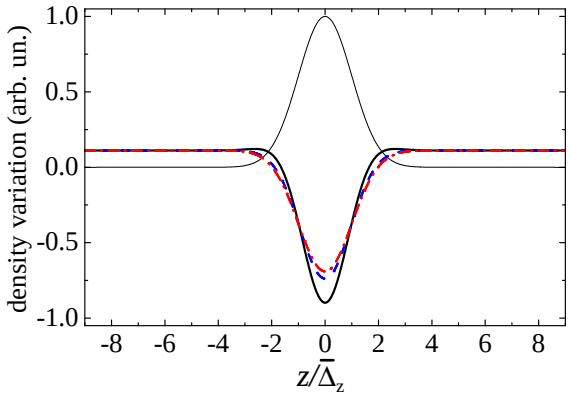

FIG. 4. (Color online) Same as in Fig. 1 but for the relaxation-time model in Eq. (98) (see text).

tral peak, and (ii) of the two positive external regions.[62] By significantly increasing the value of $\overline{\Delta}_z$ (dash-dotted curves), in- and out-scattering contributions tend to coincide, which implies that their difference tends to vanish, in total agreement with the corresponding result in Fig. 1 (dash-dotted curve). This clearly shows that the local character of the Boltzmann theory (see Eq. (19)) originates from an exact cancelation between in- and out-scattering contributions, which takes place in the semiclassical limit (i.e., $\overline{\Delta}_z \to \infty$) only.

Based on the numerical results presented so far, it is easy to conclude that the impact of scattering nonlocality is intimately related to the different spatial extension of in- and out-scattering contributions. In order to better quantify the phenomenon under examination, it is useful to introduce the effective nonlocality parameter

$$\eta^{\mathrm{in/out}} = \frac{1}{\overline{\Delta}_z} \sqrt{\frac{\int z^2 \left| F^{\mathrm{in/out}}(z) \right| dz}{\int \left| F^{\mathrm{in/out}}(z) \right| dz}} \,. \qquad (100)$$

According to its definition, this dimensionless parameter can be regarded as the standard deviation of the spatial density variation $F^{\mathrm{in/out}}(z)$ (see Eq. (93)) in units of $\overline{\Delta}_z$. It follows that when the shape of the density variation $F^{\mathrm{in/out}}(z)$ tends to the initial Gaussian profile (see dash-dotted curves in Fig. 2), the nonlocality parameter $\eta^{\mathrm{in/out}}$ in (100) tends to one; moreover, for charge variations wider than the initial distribution (see solid and dashed curves in Fig. 2a) the nonlocality parameter is expected to be greater than one, while for charge variations sharper than the initial distribution (see solid and dashed curves in Fig. 2b) the latter is expected to be smaller than one.

This scenario is fully confirmed by the numerical results reported in Fig. 3, where the nonlocality parameter in (100) is plotted as a function of $\overline{\Delta}_z$ for both in- and out-scattering contributions (here, the two curves have been obtained repeating our numerical calculation for a large set of $\overline{\Delta}_z$ values). As we can see, in the presence of a strong spatial confinement ($\overline{\Delta}_z = 5$ nm) (see solid curves in Fig. 2) the nonlocality parameter of the in-scattering term is definitely greater than one, while for the out-scattering term the latter is significantly smaller than one. By increasing the value of $\overline{\Delta}_z$, the difference between in- and out-parameters is progressively reduced, and for $\overline{\Delta}_z = 50$ nm (see dash-dotted curves in Fig. 2) their value is already very close to unity.

The bulk-GaN simulated experiments presented so far allows one to draw two basic conclusions: (i) in the presence of a nanometric spatial confinement one deals with a significant carrier-phonon scattering nonlocality (see solid curve in Fig. 1); (ii) opposite to other simplified scattering models (see below), our Lindblad superoperator (see Eq. (89)) is able to properly reproduce the semiclassical-limit behavior (see dash-dotted curve in Fig. 1), thus recovering the local character of the Boltzmann collision term (see Eq. (19)).

At this point it is crucial to compare the action of the Lindblad scattering superoperator (89) (see Fig. 1) with that of simplified dissipation models, and in particular with the conventional relaxation-time approximation. Figure 4 shows the initial time derivative of the spatial carrier density induced by the relaxation-time model in (98) as a function of the relative coordinate $z/\overline{\Delta}_z$ for the same three values of the localization parameter $\overline{\Delta}_z$ considered in Fig. 1. As we can see, also for the case of the relaxation-time model one deals with significant nonlocality effects. However, comparing Fig. 4 with Fig. 1, it is easy to recognize strong differences between the Lindblad treatment and the relaxation-time approximation: opposite to the Lindblad-superoperator results of Fig. 1, here the shape and amplitude of the charge-density variation is not strongly influenced by the value of $\overline{\Delta}_z$; more importantly, while in Fig. 1 the positive regions are spatially localized (i.e., they display a maximum and then vanish at large distances), here the charge variation tends to a constant and $\overline{\Delta}_z$-independent value. This constitutes an unambiguous proof of the intrinsic limitations of the relaxation-time approximation; indeed, opposite to the Lindblad-superoperator treatment, the latter (i) comes out to be totally non-local (as confirmed by its nearly constant values at large coordinate values),[63] and (ii) in the semiclassical limit ($\overline{\Delta}_z \to \infty$) it is intrinsically unable to reproduce the local character of the Boltzmann collision term (see Eq. (19)).

As we shall see, the totally non-local character of the relaxation-time model may give rise to a strong overestimation of the scattering-induced quantum diffusion (see Fig. 7 below).

2. *Quantum diffusion: single-particle versus scattering dynamics*

So far our focus has been devoted to the investigation of the spatial nonlocality induced by carrier-LO phonon coupling. However, in order to establish how such scattering-induced charge redistribution will affect the overall diffusion process, it is imperative to perform a time-dependent analysis including single-particle as well as scattering dynamics.

Figure 5 displays the sub-picosecond time evolution of the spatial carrier density corresponding to the initial mixed state in (96) with $\overline{\Delta}_z = 10\,\text{nm}$, obtained in the absence of carrier-phonon coupling (upper panel), via the Lindblad scattering superoperator in (89) (central panel), and via the relaxation-time model in (98) (lower panel). As we can see, compared to the scattering-free case (upper panel), both Lindblad and relaxation-time treatments give rise to a speed up of the diffusion process, and the effect is more pronounced in the relaxation-time case (lower panel).

Such ultrafast diffusion dynamics is the result of a highly non-trivial interplay between the single-particle and scattering contributions in (86); indeed, it is well

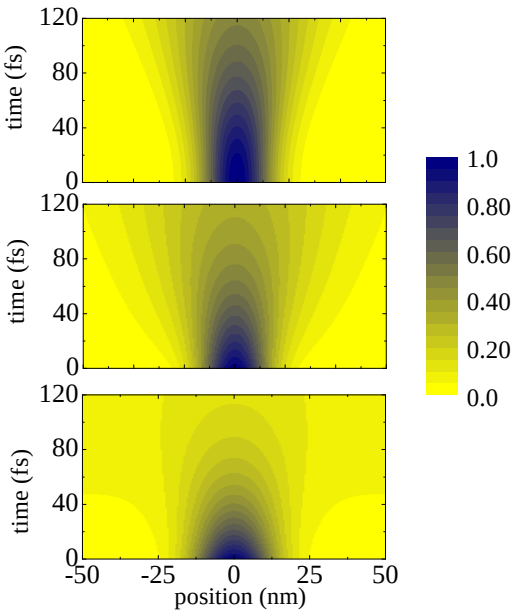

FIG. 5. (Color online) Room-temperature quantum-diffusion dynamics in a GaN bulk system obtained in the absence of carrier-phonon coupling (upper panel), via the Lindblad scattering superoperator in Eq. (89) (central panel), and via the relaxation-time model in Eq. (98) (lower panel): sub-picosecond time evolution of the spatial carrier density corresponding to the initial mixed state in Eq. (96) with $\overline{\Delta}_z = 10\,\text{nm}$ (see text).

known that also in the presence of a spatially local (i.e., Boltzmann) scattering model (for which the contribution in (88) is always equal to zero) any scattering-induced carrier redistribution tends to speed up the diffusion process.[54] In order to better evaluate the genuine diffusion contribution due to scattering nonlocality, it is then crucial to start our simulated experiments from a thermalized carrier distribution; this has been realized adopting the initial state in (96); indeed, for a parabolic-band bulk system (as the one considered here) in the absence of scattering nonlocality, the time evolution of the spatial carrier density is described by the following (time-dependent) Gaussian distribution (see upper panel in Fig. 5)

$$n(z,t) \propto \frac{e^{-\frac{z^2}{2\Delta_z^2(t)}}}{\sqrt{2\pi}\Delta_z(t)} \tag{101}$$

with

$$\Delta_z(t) = \overline{\Delta}_z \sqrt{1 + \frac{t^2}{\tau_d^2}}\ , \tag{102}$$

where

$$\tau_d = \frac{m^* \overline{\Delta}_z}{\overline{\Delta}_p} \tag{103}$$

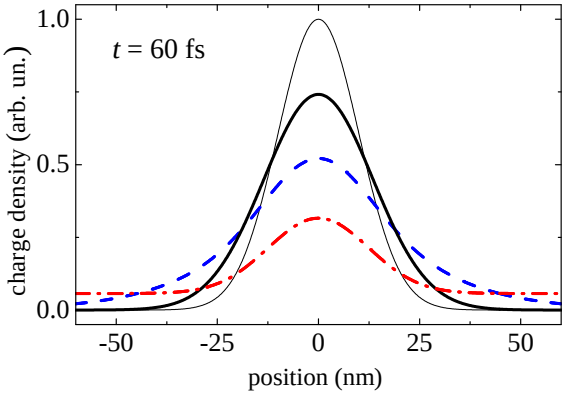

FIG. 6. (Color online) Spatial carrier-density profiles at $t = 60$ fs corresponding to the three simulated experiments of Fig. 5. Here, the scattering-free solution (solid curve) (corresponding to the local-scattering dynamics in Eq. (101)) is compared to the corresponding results obtained adopting as scattering models the Lindblad superoperator in Eq. (89) (dashed curve) as well as the relaxation-time model in Eq. (98) (dash-dotted curve); the initial distribution (thin solid curve) is also shown (see text).

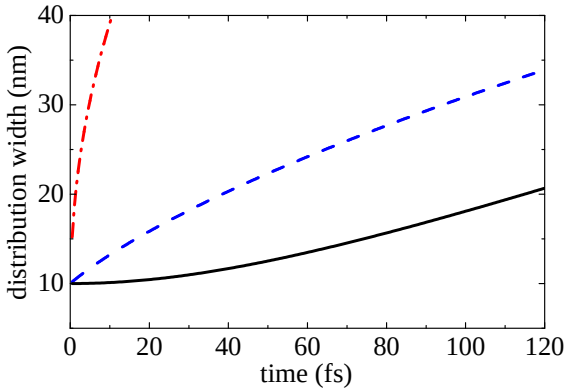

FIG. 7. (Color online) Effective spatial-distribution width λ in Eq. (104) as a function of time. Here, the local-scattering result (see Eq. (101)) (solid curve) is compared to the corresponding results obtained adopting as scattering models the Lindblad superoperator in Eq. (89) (dashed curve) as well as the relaxation-time model in Eq. (98) (dash-dotted curve) (see text).

describes the typical time scale of the scattering-free diffusion process (for the case of Fig. 5 the latter is about 70 fs).

In order to better quantify the impact of scattering-induced diffusion, in Fig. 6 the local-scattering spatial density at $t = 60$ fs (solid curve) is compared to the corresponding results obtained adopting as scattering models the Lindblad superoperator (89) (dashed curve) as well as the relaxation-time model (98) (dash-dotted curve). As already pointed out in Fig. 5, both scattering treatments give rise to a diffusion speed up, and the effect is particularly pronounced for the case of the relaxation-time model (see dash-dotted curve).

The physical origin and relative magnitude of such diffusion speed up can be easily understood in terms of the scattering-induced nonlocality previously investigated. Indeed, for both the Lindblad (Fig. 1) and the relaxation-time model (Fig. 4), carrier-phonon scattering induces a progressive charge transfer from the initial peak toward outer regions, which results in an overall spatial broadening. As already pointed out, the impact of such scattering-induced diffusion is expected to be particularly pronounced in the case of the relaxation-time model, since the latter is totally non-local (see Fig. 4). Such highly non physical behavior gives rise to an increased dissipation/decoherence dynamics, which in turn results in the significant overestimation of the diffusion process reported in the lower panel of Fig. 5.

To quantify the amount of extra diffusion reported in Figs. 5 and 6, let us introduce the effective carrier distribution width

$$\lambda = \sqrt{\frac{\int z^2 n(z)\, dz}{\int n(z)\, dz}} \ . \tag{104}$$

Figure 7 shows the time evolution of the above effective distribution width λ. Here, the local-scattering result $\lambda = \Delta_z(t)$ (solid curve) is compared to the corresponding results obtained adopting as scattering models the Lindblad superoperator (89) (dashed curve) as well as the relaxation-time model (98) (dash-dotted curve). As expected, the relaxation-time model gives rise to a strong overestimation of the diffusion process (see dash-dotted curve) compared to the Lindblad-superoperator treatment (dashed curve).

As anticipated, the relaxation-time model in (98) does not exhibit the well established in- minus out-scattering structure of the Boltzmann collision term as well as of the Lindblad superoperator in (89); it follows that within such simplified model the decay of the inter-state phase coherence (also referred to as inter-state polarization) is not dictated by a balance between in- and out-contributions, but is determined by out-scattering contributions only, leading to an overestimation of electronic decoherence. In order to elucidate this crucial point, let us start by analyzing the explicit form of Eq. (28) for the case of the relaxation-time model in (98). By denoting with

$$\rho^{\rm i}_{\alpha_1\alpha_2}(t) = \rho_{\alpha_1\alpha_2}(t) e^{-\frac{(\epsilon_{\alpha_1}-\epsilon_{\alpha_2})t}{i\hbar}} \tag{105}$$

the single-particle density matrix written in the interaction picture, the time evolution of its non-diagonal ($\alpha_1 \neq \alpha_2$) elements is given by

$$\frac{d\rho^{\rm i}_{\alpha_1\alpha_2}}{dt} = -\frac{\Gamma_{\alpha_1}+\Gamma_{\alpha_2}}{2}\, \rho^{\rm i}_{\alpha_1\alpha_2} \ , \tag{106}$$

which shows that, in addition to the free rotation in (105), the inter-state polarization decays according to the decoherence rate $(\Gamma_{\alpha_1}+\Gamma_{\alpha_2})/2$. In contrast, by inserting into Eq. (28) the explicit form of the Lindblad superoperator (89), it is easy to get

$$\frac{d\rho^{\rm i}_{\alpha_1\alpha_2}}{dt} = (\mathcal{L}_{\alpha_1\alpha_2,\alpha_1\alpha_2} + \mathcal{L}_{\alpha_2\alpha_1,\alpha_2\alpha_1})\,\rho^{\rm i}_{\alpha_1\alpha_2} + \sum_{\alpha'_1\alpha'_2\neq\alpha_1\alpha_2} \left(e^{\frac{(\epsilon_{\alpha'_1}-\epsilon_{\alpha'_2}-\epsilon_{\alpha_1}+\epsilon_{\alpha_2})t}{i\hbar}} \mathcal{L}_{\alpha_1\alpha_2,\alpha'_1\alpha'_2}\rho^{\rm i}_{\alpha'_1\alpha'_2} + {\rm H.c.} \right) \qquad (107)$$

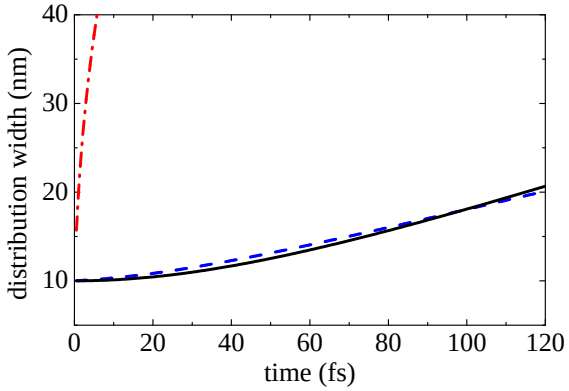

FIG. 8. (Color online) Same as in Fig. 7 but for a reduced value of the LO-phonon energy ($\epsilon_{\rm LO} = 20\,$meV) (see text).

with

$$\mathcal{L}_{\alpha_1\alpha_2,\alpha'_1\alpha'_2} = \frac{1}{2}\sum_s \left(\mathcal{P}^s_{\alpha_1\alpha_2,\alpha'_1\alpha'_2} - \delta_{\alpha_2\alpha'_2} \sum_{\alpha'} \mathcal{P}^{s*}_{\alpha'\alpha',\alpha_1\alpha'_1} \right) . \qquad (108)$$

In the presence of strongly nonelastic interaction processes, the overall impact of the second term in (107) is strongly reduced thanks to the fast temporal oscillations of the various free-rotation phase factors; moreover, taking into account that in such nonelastic-interaction limit $\mathcal{P}^s_{\alpha\alpha',\alpha\alpha'} \to 0$, one gets

$$\mathcal{L}_{\alpha\alpha',\alpha\alpha'} \to -\Gamma_\alpha/2\ , \qquad (109)$$

which implies that in this limit the Lindblad-model equation in (107) reduces to the relaxation-time one in (106). In contrast, in the presence of quasielastic processes one deals with a significant cancelation between in- and out-scattering contributions, not accounted for by the relaxation-time equation (106). It is worth stressing that such intrinsic limitation of relaxation-time models has been already recognized in the analysis of ultrafast phenomena in photoexcited semiconductors[12], showing that the latter becomes particularly severe for the case of quasielastic processes.[64]

To confirm this physical interpretation, we have repeated the simulated experiments presented so far artificially reducing the GaN LO-phonon energy by a factor 4 (from 80 to 20 meV), such to mimic the quasielastic-process limit. The time evolution of the effective distribution width λ corresponding to these new simulations is reported in Fig. 8. As expected, compared to the results reported in Fig. 7, the decoherence overestimation produced by the relaxation-time model (dash-dotted curve) is significantly increased, while the diffusion speed up

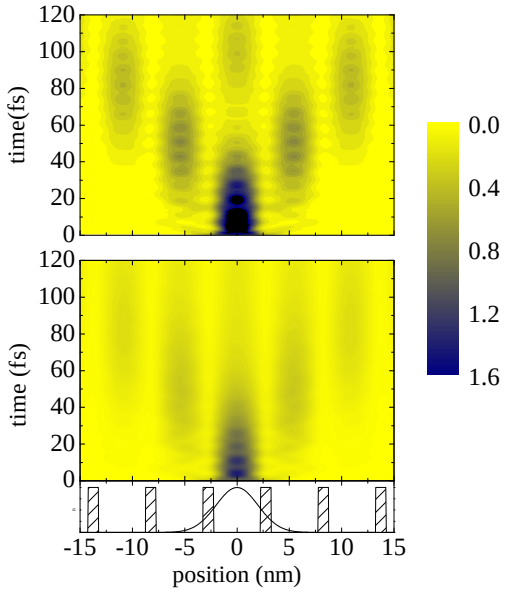

FIG. 9. (Color online) Room-temperature quantum-diffusion dynamics in a GaN-based superlattice (lower panel) (band offset of 0.3 eV and well and barrier widths of 4.5 and 1 nm) obtained in the absence of carrier-phonon coupling (upper panel) and via the Lindblad scattering superoperator in Eq. (89) (central panel): sub-picosecond time evolution of the spatial carrier density corresponding to the initial mixed state in Eq. (96) with $\overline{\Delta}_z = 2\,$nm (see text).

induced by the Lindblad superoperator (dashed curve) is strongly reduced. Indeed, in spite of the fact that the LO-phonon energy is still significantly different from zero, the effect of phonon scattering is already negligible. This is a clear indication that in the presence of genuine quasi elastic processes like, e.g., carrier-acoustic phonons or carrier-carrier scattering (i) the relaxation-time model is definitely inadequate, and (ii) quantum diffusion due to scattering nonlocality is expected to play a minor role.

C. From bulk systems to nanostructures

As a final set of simulated experiments aimed at showing the power and flexibility of the proposed density-matrix approach, we have extended the bulk-system analysis presented so far to the case of a periodic nanostructure. Figure 9 displays the sub-picosecond time evolution of the spatial carrier density in a GaN-based superlattice (see lower panel) corresponding to the initial mixed state in (96) with $\overline{\Delta}_z = 2\,$nm, obtained in the scattering-free case (upper panel) and employing the Lindblad scattering superoperator in (89) (central panel). Compared to

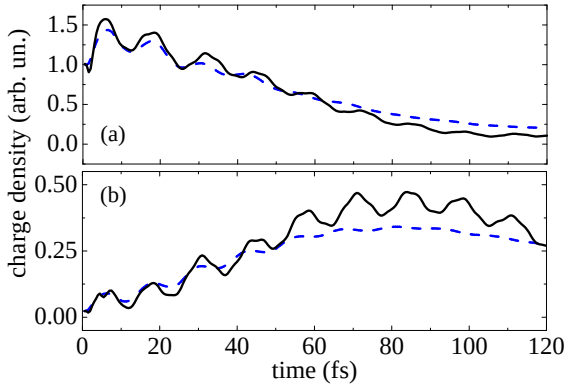

FIG. 10. (Color online) Time evolution of the carrier population in the central well of the superlattice (panel a) as well as in the two adjacent wells (panel b) corresponding to the scattering-free simulation (solid curves (upper panel in Fig. 9)) and to the Lindblad-scattering simulation (dashed curves (central panel in Fig. 9)) (see text).

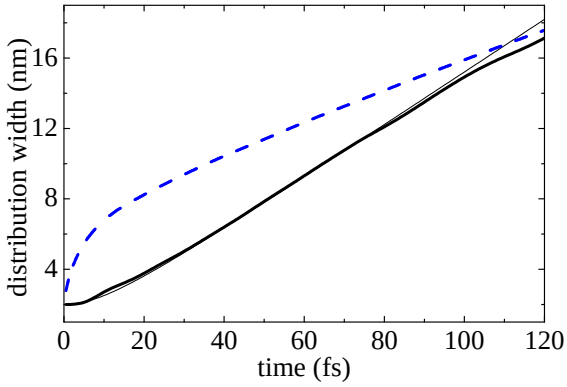

FIG. 11. (Color online) Effective spatial-distribution width λ in Eq. (104) as a function of time. Here, the local-scattering bulk result in Eq. (101) (thin solid curve) is compared to the scattering-free superlattice result (solid curve corresponding to the upper-panel result of Fig. 9) as well as to the Lindblad-scattering superlattice result (dashed curve corresponding to the central-panel result of Fig. 9) (see text).

the corresponding bulk-system results of Fig. 5, here the presence of the superlattice structure (see lower panel) gives rise to a non-trivial interplay between the spatial quantum confinement dictated by the nanostructure potential profile and the scattering-induced diffusion, resulting in a superlattice-induced modulation of the density profile.

In the absence of carrier-phonon scattering (upper panel) one deals with coherent charge oscillations originating from the diffusion dynamics of the initial packet through the superlattice structure. In particular, it is easy to recognize the typical signature of inter-well coherent tunneling, a peculiar phenomenon in coupled quantum-well structures.[22] To better elucidate this crucial feature, in Fig. 10 we have reported the time evolution of the carrier population in the central well of the superlattice (panel a) as well as in the two adjacent wells (panel b). As we can see, in the scattering-free case (solid curves corresponding to the upper-panel result of Fig. 9) one deals with a significant charge transfer from the central well toward the adjacent ones and vice versa, the so-called coherent-tunneling dynamics. However, compared to simple two-well systems, here the situation is by far more complicated: once a fraction of the central-well charge has reached the adjacent wells, part of it will be transferred back to the central well, but also to the external nearest-neighbor ones; this process will progressively extend to an increasing number of wells, giving rise to the quantum-mechanical diffusion process displayed in the upper panel of Fig. 9.

In the presence of carrier-LO phonon scattering (see central panel in Fig. 9), the fully coherent dynamics just described is strongly suppressed; indeed, the significant temporal oscillations in Fig. 10 are strongly reduced, giving rise at long times to a classical-like diffusion scenario typical of a so-called incoherent-tunneling dynamics.[22]

Finally, it is important to point out that in the presence of energy dissipation the interplay between single-particle phase coherence (dictated by the superlattice potential profile) and phonon-induced decoherence (dictated by the Lindblad scattering superoperator) is highly non trivial. This is clearly shown in Fig. 11, where we report the effective spatial-distribution width λ in (104) corresponding to the two simulated experiments of Fig. 9.

As we can see, the scattering-free diffusion dynamics within the superlattice structure (solid curve) does not differ significantly from the corresponding bulk result (thin solid curve). In contrast, at short times (less than 100 fs) the presence of carrier-LO phonon scattering (dashed curve) gives rise to a significant diffusion speed up (compared to the scattering-free result (solid curve)); at longer times the non-local action of the scattering superoperator vanishes, and at the end of the simulation the spatial broadening induced by the Lindblad superoperator comes out to be even smaller than the scattering-free one. Such non-trivial behavior can be explained as follows: at short times the strong spatial localization of the initial distribution induces a significant diffusion speed up due to carrier-phonon nonlocality effects; at longer times such scattering-induced nonlocality is strongly reduced, and, at the same time, energy dissipation tends to destroy inter-state phase coherence, thus limiting the diffusion process compared to the scattering-free case.

Generally speaking, we finally stress that the ability of investigating such space dependent phenomena originating from the complex interplay between single-particle quantum coherence and phonon-induced energy dissipation versus decoherence —definitely not possible via Boltzmann-like Monte Carlo simulation schemes— constitutes a distinguished feature of the proposed quantum mechanical treatment.

VI. SUMMARY AND CONCLUSIONS

In this paper we have provided a rigorous treatment of scattering-induced spatial nonlocality in bulk as well as in nanostructured materials.

On the one hand, starting from the conventional density-matrix formalism and employing as ideal instrument for the study of the semiclassical limit the well-known Wigner-function picture, we have performed a fully quantum-mechanical derivation of the space-dependent Boltzmann equation.

On the other hand, we have analyzed the validity limits of such semiclassical approximation scheme, pointing out, in particular, regimes where scattering-nonlocality effects may play a relevant role; to this end we have supplemented our analytical investigation with a relevant set of simulated experiments, discussing and further expanding preliminary studies of scattering-induced quantum diffusion in GaN-based nanomaterials recently presented in Ref. 38.

Our numerical investigation of ultrafast space-dependent phenomena in GaN bulk allows one to draw the following conclusions.

In the presence of carrier localization on the nanometric space scale (see Fig. 1) within the proposed Lindblad treatment one deals with significant phonon-induced nonlocality effects; our analysis has shown that such nonlocal character is the result of a different spatial localization of in- and out-scattering contributions (see Figs. 2 and 3); these nonlocality effects will progressively vanish as the carrier delocalization increases, thus recovering, as expected (see Sec. IV C), the local character of the Boltzmann collision term.

A detailed comparison of the proposed Lindblad scattering model (see Fig. 1) with the conventional relaxation-time approximation (see Fig. 4), has shown that the latter (i) leads to a significant overestimation of phonon-induced decoherence as well as scattering nonlocality, and (ii) is intrinsically unable to reproduce the local character of the Boltzmann collision term.

Thanks to our time-dependent simulations, we have shown that in GaN bulk systems one deals with a relevant competition between free-particle diffusion and phonon-induced non-local effects, giving rise to a global diffusion speed up (see Figs. 5 and 6); once again, a comparison between the proposed Lindblad treatment and the relaxation-time model has clearly shown that the latter leads to a significant overestimation of such diffusion speed up (see Fig. 7), and that this limitation is particularly severe for the case of quasielastic dissipation processes (see Fig. 8).

Moving from bulk systems to periodically modulated nanostructures, the interpretation of the diffusion process in the presence of phonon-induced dissipation is by far more complicated. Indeed, compared to the bulk-system results (see Fig. 5), the presence of the superlattice structure (see Figs. 9 and 10) gives rise to a non-trivial interplay between the spatial quantum confinement dictated by the nanostructure potential profile and the scattering-induced diffusion, resulting in a superlattice-induced modulation of the density profile. In particular, the scattering-free diffusion dynamics within the superlattice structure does not differ significantly from the corresponding bulk result (see Fig. 11); in contrast, at short times the presence of carrier-LO phonon scattering gives rise to a significant diffusion speed up, but at longer times the non-local action of the scattering superoperator vanishes, and at the end of the simulation the spatial broadening induced by the Lindblad superoperator comes out to be even smaller than the scattering-free one.

Let us finally stress that in the presence of particularly strong interaction mechanisms as well as of extremely short electromagnetic excitations, the application of the Markov limit becomes questionable;[12,13] however, for a wide range of nanodevices and operation conditions the proposed Markov treatment is expected to well reproduce the sub-picosecond dynamics induced by a large variety of single-particle scattering mechanisms.

ACKNOWLEDGMENTS

We are extremely grateful to Rita Claudia Iotti for stimulating and fruitful discussions.

We gratefully acknowledge funding by the Graphene@PoliTo laboratory of the Politecnico di Torino, operating within the European FET-ICT Graphene Flagship project (www.graphene-flagship.eu).

* Fausto.Rossi@polito.it; staff.polito.it/Fausto.Rossi

[1] L. Esaki and R. Tsu, IBM J. Res. Dev. **14**, 61 (1970).
[2] T. Ihn, *Semiconductor Nanostructures: Quantum States and Electronic Transport* (OUP Oxford, 2010).
[3] C. Liu, J. Sun, J. Tang, and P. Yang, Nano Lett. **12**, 5407 (2012).
[4] Y. Cheng and R. Beresford, Nano Lett. **13**, 614 (2013).
[5] S. J. LeBlanc, M. R. McClanahan, M. Jones, and P. J. Moyer, Nano Lett. **13**, 1662 (2013).
[6] F. Capasso, *Physics of Quantum Electron Devices*, Springer Series in Electronics and Photonics (Springer London, Limited, 2011).
[7] G. Bastard, *Wave mechanics applied to semiconductor heterostructures*, Monographies de physique (Les Éditions de Physique, 1988).
[8] C. Jacoboni and P. Lugli, *The Monte Carlo Method for Semiconductor Device Simulation* (Springer, 1989).
[9] W. R. Frensley, Rev. Mod. Phys. **62**, 745 (1990).
[10] V. M. Axt and S. Mukamel, Rev. Mod. Phys. **70**, 145 (1998).

[11] S. Datta, Superlattice. Microst. **28**, 253 (2000).
[12] F. Rossi and T. Kuhn, Rev. Mod. Phys. **74**, 895 (2002).
[13] V. M. Axt and T. Kuhn, Rep. Prog. Phys. **67**, 433 (2004).
[14] A. Pecchia and A. Di Carlo, Rep. Prog. Phys. **67**, 1497 (2004).
[15] R. C. Iotti and F. Rossi, Rep. Prog. Phys. **68**, 2533 (2005).
[16] K. De Greve, L. Yu, P. L. McMahon, J. S. Pelc, C. M. Natarajan, N. Y. Kim, E. Abe, S. Maier, C. Schneider, M. Kamp, S. Hoefling, R. H. Hadfield, A. Forchel, M. M. Fejer, and Y. Yamamoto, Nature **491**, 421 (2012).
[17] W. B. Gao, P. Fallahi, E. Togan, J. Miguel-Sanchez, and A. Imamoglu, Nature **491**, 426 (2012).
[18] F. J. Garcia de Abajo, Science **339**, 917 (2013).
[19] E. S. Reich, Nature **497**, 422 (2013).
[20] F. Rossi, *Theory of Semiconductor Quantum Devices: Microscopic Modeling and Simulation Strategies* (Springer, 2011).
[21] M. Ryzhii and V. Ryzhii, Appl. Phys. Lett. **72**, 842 (1998).
[22] R. C. Iotti and F. Rossi, Phys. Rev. Lett. **87**, 146603 (2001).
[23] R. Köhler, A. Tredicucci, F. Beltram, H. E. Beere, E. H. Linfield, A. G. Davies, D. A. Ritchie, R. C. Iotti, and F. Rossi, Nature **417**, 156 (2002).
[24] H. Callebaut, S. Kumar, B. S. Williams, Q. Hu, and J. L. Reno, Appl. Phys. Lett. **84**, 645 (2004).
[25] J. T. Lu and J. C. Cao, Appl. Phys. Lett. **89**, 211115 (2006).
[26] E. Bellotti, K. Driscoll, T. D. Moustakas, and R. Paiella, Appl. Phys. Lett. **92**, 101112 (2008).
[27] C. Jirauschek, Appl. Phys. Lett. **96**, 011103 (2010).
[28] A. Matyas, M. A. Belkin, P. Lugli, and C. Jirauschek, Appl. Phys. Lett. **96**, 201110 (2010).
[29] R. C. Iotti, F. Rossi, M. S. Vitiello, G. Scamarcio, L. Mahler, and A. Tredicucci, Appl. Phys. Lett. **97**, 033110 (2010).
[30] M. S. Vitiello, R. C. Iotti, F. Rossi, L. Mahler, A. Tredicucci, H. E. Beere, D. A. Ritchie, Q. Hu, and G. Scamarcio, Appl. Phys. Lett. **100**, 091101 (2012).
[31] A. Matyas, P. Lugli, and C. Jirauschek, Appl. Phys. Lett. **102**, 011101 (2013).
[32] R. C. Iotti and F. Rossi, New J. Phys. **15**, 075027 (2013).
[33] C. Gmachl, F. Capasso, D. L. Sivco, and A. Y. Cho, Rep. Prog. Phys. **64**, 1533 (2001).
[34] R. Brunetti, C. Jacoboni, and P. J. Price, Phys. Rev. B **50**, 11872 (1994).
[35] D. Reiter, M. Glanemann, V. M. Axt, and T. Kuhn, Phys. Rev. B **75**, 205327 (2007).
[36] R. Rosati and F. Rossi, Appl. Phys. Lett. **103**, 113105 (2013).
[37] D. Taj, R. C. Iotti, and F. Rossi, Eur. Phys. J. B **72**, 305 (2009).
[38] R. Rosati and F. Rossi, EPL **105**, 17010 (2014).
[39] R. Kubo and N. Saito, *Statistical Physics I: Equilibrium Statistical Mechanics*, Springer Series in Solid-state Sciences (Springer London, Limited, 2012).
[40] R. Kubo and N. Hashitsume, *Statistical Physics II: Nonequilibrium Statistical Mechanics*, Springer Series in Solid-state Sciences (Springer London, Limited, 2012).
[41] C. Zachos, D. Fairlie, and T. Curtright, *Quantum Mechanics in Phase Space: An Overview with Selected Papers*, World Scientific series in 20th century physics (World Scientific, 2005).
[42] A. Burshtein, *Introduction to Thermodynamics and Kinetic Theory of Matter*, Physics textbook (Wiley, 2008).
[43] G. Kremer, *An Introduction to the Boltzmann Equation and Transport Processes in Gases*, Interaction of Mechanics and Mathematics (Springer, 2010).
[44] C. Cercignani, *The Boltzmann Equation and Its Applications*, Applied Mathematical Sciences (Springer London, Limited, 2012).
[45] L. Boltzmann, *Lectures on Gas Theory*, Dover Books on Physics (Dover Publications, 2012).
[46] C. Jacoboni, *Theory of Electron Transport in Semiconductors: A Pathway from Elementary Physics to Nonequilibrium Green Functions* (Springer, 2010).
[47] It is worth mentioning that an alternative approach, equivalent to the density-matrix formalism considered in this Paper, is given by the well-known nonequilibrium Green's-function technique. An introduction to the theory of nonequilibrium Green's functions with applications to many problems in transport and optics of semiconductors can be found in the book by Hartmut Haug and Antti-Pekka Jauho;[65] by employing – and further developing and extending – such nonequilibrium Green's function formalism, a number of groups have proposed efficient quantum-transport treatments for the study of various meso- and nanoscale structures as well as of corresponding micro- and optoelectronic devices (see, e.g., Ref. 66).
[48] R. C. Iotti, E. Ciancio, and F. Rossi, Phys. Rev. B **72**, 125347 (2005).
[49] G. Lindblad, Commun. Math. Phys. **48**, 119 (1976).
[50] H. Haug and S. Koch, *Quantum Theory of the Optical and Electronic Properties of Semiconductors* (World Scientific, 2004).
[51] O. Hess and T. Kuhn, Phys. Rev. A **54**, 3347 (1996).
[52] L. Demeio, P. Bordone, and C. Jacoboni, Transport Theor. Stat. **34**, 499 (2005).
[53] R. Rosati, F. Dolcini, R. C. Iotti, and F. Rossi, Phys. Rev. B **88**, 035401 (2013).
[54] N. Ashcroft and N. Mermin, *Solid State Physics* (Cengage Learning India Private Limited, 2011).
[55] As recently pointed out,[53,67–69] the Wigner-function formalism applied to the modeling of open quantum devices may lead to highly unphysical results, mainly ascribed to the failure of the conventional spatial boundary-condition scheme applied to the Wigner transport equation. It is however imperative to stress that such limitations do not apply to the Wigner-function analysis presented below, since the latter refers to an infinitely extended system and not to a quantum device with open spatial boundaries.
[56] F. Buot, *Nonequilibrium quantum transport physics in nanosystems: foundation of computational nonequilibrium physics in nanoscience and nanotechnology* (World Scientific, 2009).
[57] Such envelope-function Hamiltonian can be regarded as the quantum-mechanical generalization of the semiclassical Hamiltonian in (6).
[58] R. Feynman, A. Hibbs, and D. Styer, *Quantum Mechanics and Path Integrals*, Dover books on physics (Dover Publications, Incorporated, 2010).
[59] R. Gebauer and R. Car, Phys. Rev. Lett. **93**, 160404 (2004).
[60] J. E. Moyal and M. S. Bartlett, Math. Proc. Cambridge Phil. Soc. **45**, 99 (1949).
[61] F. Dolcini, R. C. Iotti, and F. Rossi, Phys. Rev. B **88**, 115421 (2013).
[62] It is worth stressing that, in view of the trace-preserving character of the Lindblad superoperator (25), the total car-

rier density (i.e., integrated over the spatial coordinate z) is preserved; this implies that the positive and negative regions in Fig. 1 should cancel each other out.

[63] Indeed, for the relaxation-time model in (98) it is not possible to introduce a nonlocality parameter (see Eq. (100)), since the spatial standard deviation of the charge-density variation in Fig. 4 is always infinite.

[64] F. Rossi, S. Haas, and T. Kuhn, Phys. Rev. Lett. **72**, 152 (1994).

[65] H. Haug and A. Jauho, *Quantum Kinetics in Transport and Optics of Semiconductors* (Springer, 2007).

[66] S. Datta, *Quantum Transport: Atom to Transistor* (Cambridge University Press, 2005).

[67] D. Taj, L. Genovese, and F. Rossi, Europhys. Lett. **74**, 1060 (2006).

[68] A. Savio and A. Poncet, J. Appl. Phys. **109**, 033713 (2011).

[69] C. Jacoboni and P. Bordone, J. Comput. Electron. 10.1007/s10825-013-0510-7.